

ASSESSING SPATIAL DISPARITIES: A BAYESIAN LINEAR REGRESSION APPROACH

KYLE LIN WU AND SUDIPTO BANERJEE

ABSTRACT. Epidemiological investigations of regionally aggregated spatial data often involve detecting spatial health disparities among neighboring regions on a map of disease mortality or incidence rates. Analyzing such data introduces spatial dependence among health outcomes and seeks to report statistically significant spatial disparities by delineating boundaries that separate neighboring regions with disparate health outcomes. However, there are statistical challenges to appropriately define what constitutes a spatial disparity and to construct robust probabilistic inferences for spatial disparities. We enrich the familiar Bayesian linear regression framework to introduce spatial autoregression and offer model-based detection of spatial disparities. We derive exploitable analytical tractability that considerably accelerates computation. Simulation experiments conducted on a county map of the entire United States demonstrate the effectiveness of our method, and we apply our method to a data set from the Institute of Health Metrics and Evaluation (IHME) on age-standardized US county-level estimates of lung cancer mortality rates.

1. INTRODUCTION

We develop statistical methods for detecting local spatial disparities on maps. Disparities in health outcomes are a rapidly evolving field within public health ([Rao, 2023](#)) and spatial variation in health outcomes affects how disparities manifest on disease maps. Spatial data analysis in epidemiological investigations is extensively documented ([Lawson, 2013](#); [Lawson et al., 2016](#); [Waller and Carlin, 2010](#); [Waller and Gotway, 2004](#)). Inference on disparities proceeds from “difference boundaries” that represent significant differences between neighbors and delineate regions with significantly different disease mortality and incidence rates, helping to improve the geographic allocation of health care resources and guide future investigation into local determinants. Boundary detection enables precise identification of health event clusters and sudden changes in latent or observed environmental exposures, which is crucial for defining sampling protocols across a diverse range of health environments and planning targeted interventions ([Copeland, 2010](#); [Jacquez, 2010](#)). For example, [Barboza-Salerno et al. \(2025\)](#) apply boundary detection to identify local socioeconomic inequalities and estimate their association with neighborhood child mortality. In geographic analysis, the problem is often called “wombling” (see [Jacquez and Greiling, 2003aa, 2003bb](#); [Fitzpatrick et al. \(2010\)](#); [Li et al. \(2011\)](#); [Lu and Carlin \(2005\)](#); [Ma and Carlin \(2007\)](#)).

for some algorithmic approaches with applications). Probabilistic model-based approaches include developments in [Corpas-Burgos and Martinez-Beneito \(2020\)](#); [Gao et al. \(2023\)](#); [Hanson et al. \(2015\)](#); [Lee and Mitchell \(2012\)](#); [Li et al. \(2012, 2015\)](#); [Lu et al. \(2007\)](#); [Ma et al. \(2010\)](#) and [Aiello and Banerjee \(2025\)](#).

The aforementioned articles present an impressive range of methods, but are broadly classified into two groups. The first embraces hierarchical models and Bayesian inference for the spatial adjacency matrix by modeling its elements. The second endows the spatial random effects with a probability law that accommodates nonzero probabilities on neighboring spatial random effects being equal (often using an areal Dirichlet process or some adaptation thereof), which are computed as posterior probabilities. Both groups introduce spatial dependence and aim to balance the underlying spatial similarities with the ability to detect differences among neighbors. Our current contribution offers a computationally scalable and analytically tractable approach to this problem. Instead of modeling spatial effects as realizations of a Dirichlet process, which struggles to learn from the data and impedes convergence of iterative estimation algorithms, we devise fully model-based Bayesian inference within an augmented spatial linear regression framework. More specifically, we treat spatial disparities as a multiple comparison problem within a Bayesian inferential paradigm by testing for differences in spatial random effects between neighboring regions. Subsequently, we use posterior probabilities of such differences to detect spatial disparities while controlling a Bayesian false discovery rate or FDR ([Müller et al., 2007](#)). Controlling the false discovery rate is preferred to controlling the family wise error rate or false positive rate because it offers increased power and flexibility ([Catelan and Biggeri, 2010](#); [Glickman et al., 2014](#)) and has been previously applied in analyses of health disparities ([Slutske et al., 2023](#); [Tian et al., 2010](#)). Further developments of Bayesian FDR for multiple testing in spatial settings include [Sun et al. \(2015\)](#); [Tansey et al. \(2018\)](#); [Ventrucci et al. \(2011\)](#).

Benefits of our approach include clearer interpretation of spatial effects, computational simplicity, accounting for small differences in the values of neighboring spatial effects in determining spatial disparity, and providing improved sensitivity and specificity for detecting boundary differences (as seen in [Gao et al., 2023](#)). Our parametric approach is suitable for applications where one disease map is of interest and lack of replication hinders non-parametric methods (such as in [Jagai et al., 2017](#); [Rodriguez et al., 2018](#); [Slack et al., 2014](#)).

We exploit closed-form distribution theory to account for the differences between the values of the spatial effects and evaluate posterior probabilities of such differences exceeding a certain threshold. We extend [Lu and Carlin \(2005\)](#) and [Fitzpatrick et al. \(2010\)](#), who use only posterior means or spatial residuals to detect differences, to fully model-based inference. We provide an outline for the rest of the article. Section 2 discusses the problem of detecting differences between fixed effects in a linear model before we extend to spatial random effects. Section 3 develops the notion of a difference boundary, demonstrates a meaningful connection to traditional hypothesis testing in the simple linear regression model, and considers extensions to a generalized linear

model. Section 4 evaluates our methods alongside an existing Bayesian nonparametric approach using simulated data over a map of Californian counties followed by an analysis of lung cancer mortality data in Section 5. Section 6 concludes with a brief discussion.

2. ASSESSING CONTRASTS IN BAYESIAN LINEAR REGRESSION

2.1. Random Effects under an Augmented Linear System. We follow the adaptation by [Riebler et al. \(2016\)](#) of the “BYM” model ([Besag et al., 1991](#)) to ensure identifiable parameters and provide better interpretation. The “BYM2” model is

$$y = X\beta + \gamma + \eta, \quad \gamma = \sigma\sqrt{\rho}\phi, \quad \phi \sim N_n(0, V_\phi), \quad \eta = \sigma\sqrt{1-\rho}v, \quad v \sim N_n(0, I_n) \quad (1)$$

where ϕ is an $n \times 1$ vector of random effects, V_ϕ is a known positive definite matrix such that $\pi(\phi)$ is proper. The parameter σ^2 captures the overall error variance if c is set so that the geometric mean of the marginal prior variances is equal to one, and ρ represents the proportion of total variance attributed to the spatial structure ([Riebler et al., 2016](#)). For subsequent analysis, we specify a conditionally autoregressive (CAR) structure, one of the most popular spatial models used in areal data analysis. Here, $\pi(\gamma_i | \sigma^2, \gamma_j, j \neq i) = N(\alpha \sum_j w_{ij} \gamma_j / w_{i+}, c\sigma^2 / w_{i+})$, where w_{ij} is the binary adjacency indicator for regions i and j , α is a spatial smoothing parameter, c is a fixed scaling constant and $w_{i+} = \sum_j w_{ij}$ is the number of neighbors of region i . The conditional distribution of each spatial residual is based on a linear combination of its neighbors. By Brook’s lemma ([Besag et al., 1991](#)), this equates to setting $V_\phi^{-1} = c(D_W - \alpha W)$ in (1), where W is the adjacency matrix, D_W is diagonal with the diagonal elements $D_{W,ii} = w_{i+}$ ([Banerjee et al., 2015](#), Chap. 4). The density $\pi(\phi)$ is proper when $\alpha \in (1/\lambda_{\min}, 1)$, where λ_{\min} is the smallest eigenvalue of $D_W^{-1/2} W D_W^{-1/2}$. Since ρ already controls the amount of spatial smoothing in (1), we set $\alpha = 0.99$ in the following sections to improve the identifiability of spatial effects ϕ , which we consider as potential indicators of latent factors driving local health inequity.

If $\pi(\gamma, \beta, \sigma^2, \rho) = N(\gamma | 0, \sigma^2 \rho V_\phi) \times N(\beta | M_0 m_0, \sigma^2 M_0) \times \text{IG}(\sigma^2 | a_{\sigma^2}, b_{\sigma^2}) \times \pi(\rho)$ is the prior for (1), then the joint distribution arises from the augmented linear model,

$$\underbrace{\begin{bmatrix} y \\ M_0 m_0 \\ 0_n \end{bmatrix}}_{y_\star} = \underbrace{\begin{bmatrix} X & I_n \\ I_p & 0_{p \times n} \\ 0_{n \times p} & I_n \end{bmatrix}}_{X_\star} \underbrace{\begin{bmatrix} \beta \\ \gamma \end{bmatrix}}_{\gamma_\star} + \underbrace{\begin{bmatrix} \eta \\ \eta_\beta \\ \eta_\phi \end{bmatrix}}_{\eta_\star}, \quad \eta_\star \sim N_{2n+p} \left(0_{2n+p}, \sigma^2 V_{y_\star} \right), \quad (2)$$

where $V_{y_\star} = \begin{bmatrix} (1-\rho)I_n & 0 & 0 \\ 0 & M_0 & 0 \\ 0 & 0 & \rho V_\phi \end{bmatrix}$ and a prior $\pi(\gamma_\star, \sigma^2, \rho) = \text{IG}(\sigma^2 | a_{\sigma^2}, b_{\sigma^2}) \times \pi(\rho)$ (since

the prior for $\gamma_\star = (\beta^T, \gamma^T)^T$ has been absorbed into the linear system). By conjugacy of the prior $\pi(\gamma_\star, \sigma^2 | \rho)$ with the Gaussian likelihood in (2), the resulting conditional posterior joint

distribution, $\pi(\gamma_\star, \sigma^2 | y_\star, \rho) \propto \pi(y_\star | \gamma_\star, \sigma^2, \rho) \times \pi(\gamma_\star, \sigma^2 | \rho)$, is

$$\pi(\gamma_\star, \sigma^2 | y, \rho) = N_{n+p} \left(\gamma_\star | M_\star m_\star, \sigma^2 M_\star \right) \times \text{IG} \left(\sigma^2 | a_n, b_n \right), \quad (3)$$

where $M_\star = (X_\star^\top V_{y_\star}^{-1} X_\star)^{-1}$, $m_\star = X_\star^\top V_{y_\star}^{-1} y_\star = \left(\frac{1}{1-\rho} y^\top X + m_0^\top, \frac{1}{1-\rho} y^\top \right)^\top$, $a_n = a_{\sigma^2} + \frac{n}{2}$, and $b_n = b_{\sigma^2} + \frac{1}{2} \left(\frac{1}{1-\rho} y^\top y + m_0^\top M_0 m_0 - m_\star^\top M_\star m_\star \right)$. The posterior mean $M_\star m_\star = \hat{\gamma}_\star$ is the general least squares regression estimate to be solved $X_\star^\top V_{y_\star}^{-1} X_\star \hat{\gamma}_\star = X_\star^\top V_{y_\star}^{-1} y_\star$ and $b_n = b_{\sigma^2} + \frac{ns^2}{2}$, where $s^2 = \frac{1}{n} (y_\star - X_\star \hat{\gamma}_\star)^\top V_{y_\star}^{-1} (y_\star - X_\star \hat{\gamma}_\star)$ is the mean residual sums of squares from (2).

Fixing $\rho \in (0, 1)$ we can draw exact posterior samples from (3). Since $\gamma = \sigma \sqrt{\rho} \phi$, we obtain

$$\text{Var}(\phi | y, \sigma^2, \rho) = \left(V_\phi^{-1} + \frac{\rho}{1-\rho} \left(I_n - X A^{-1} X^\top \right) \right)^{-1}, \quad (4)$$

where $A = X^\top X + (1-\rho)M_0^{-1}$. A flat prior to β , that is, $M_0^{-1} = O$, yields $A = X^\top X$ and

$$\lim_{M_0^{-1} \rightarrow O} \text{Var}(\phi | y, \sigma^2, \rho) = \left(V_\phi^{-1} + \frac{\rho}{1-\rho} (I_n - H) \right)^{-1}, \quad \text{where } H = X(X^\top X)^{-1} X^\top. \quad (5)$$

Section 3.2 uses these expressions to formulate the detection of differences between boundaries.

2.2. Limiting cases. The limits of the conditional posterior distribution of (β, γ) as $\rho \rightarrow 0^+$ or as $\rho \rightarrow 1^-$ are analytically derived when the prior is non-informative on β . By spectral decomposition, $V_\phi^{1/2} (I - H) V_\phi^{1/2} = C D C^\top$ where C is an orthogonal matrix and $D = \text{diag}(d_1, \dots, d_n)$ with entries that are nonnegative eigenvalues of $V_\phi^{1/2} (I - H) V_\phi^{1/2}$. Let $U = V_\phi^{1/2} C$, then U is invertible, $U^\top V_\phi^{-1} U = I_n$, and $U^\top (I_n - H) U = D$. The block entries of M_\star and $\hat{\gamma}_\star$ in (3) reveal that as $\rho \rightarrow 0^+$,

$$\begin{aligned} \mathbb{E}[\gamma | y, \sigma^2, \rho] &= U \left(\frac{1-\rho}{\rho} I_n + D \right)^{-1} D U^{-1} y \rightarrow 0_n, \\ \text{Var}(\gamma | y, \sigma^2, \rho) &= \sigma^2 U \left(\frac{1}{\rho} I_n + \frac{1}{1-\rho} D \right)^{-1} U^\top \rightarrow 0_{n \times n}. \end{aligned} \quad (6)$$

Therefore, with a flat prior on β , $\lim_{\rho \rightarrow 0^+} \pi(\beta, \gamma, \sigma^2 | y, \rho) = \delta_{0_n}(\gamma)$ (degenerate mass at $\gamma = 0_n$).

We also obtain $\lim_{\rho \rightarrow 1^-} \left(\frac{1}{\rho} I_n + \frac{1}{1-\rho} D \right)^{-1} = I_n - D^\star$ and $\lim_{\rho \rightarrow 1^-} \left(\frac{1-\rho}{\rho} I_n + D \right)^{-1} D = D^\star$ where $D^\star \in \mathbb{R}^{n \times n}$ is diagonal with $D_{ii}^\star = I(d_i > 0)$ for $i = 1, \dots, n$. Simplifications reveal

$$\begin{aligned} \mathbb{E}[\beta | y, \sigma^2, \rho] &\rightarrow (X^\top X)^{-1} X^\top (y - U D^\star U^{-1} e), \quad \mathbb{E}[\gamma | y, \sigma^2, \rho] \rightarrow U D^\star U^{-1} e, \\ \text{Var}(\beta | y, \sigma^2, \rho) &\rightarrow \sigma^2 (X^\top X)^{-1} X^\top V X (X^\top X)^{-1}, \quad \text{Var}(\gamma | y, \sigma^2, \rho) \rightarrow \sigma^2 V, \end{aligned} \quad (7)$$

as $\rho \rightarrow 1^-$, where $e = (I - H)y$ are the residuals from ordinary least squares and $V = V_\phi - U D^\star U^\top$. Finally, $\lim_{\rho \rightarrow 1^-} b_n = b_{\sigma^2} + \frac{1}{2} v^\top D^\star v$, where $v = U^{-1} e$. Therefore, $\lim_{\rho \rightarrow 1^-} \pi(\sigma^2 | y, \rho) = \text{IG}(\sigma^2 | a_{\sigma^2} + n/2, b_{\sigma^2} + v^\top D^\star v/2)$. Section 3.5 discusses their implications for boundary detection.

3. A NEW FRAMEWORK FOR DETECTING SPATIAL DISPARITIES

3.1. Connection to Classical Hypothesis Testing. We first briefly address contrast testing in Bayesian linear regression without spatial effects, that is, $\gamma = 0$ in (1). Whereas $\mathbb{P}(c_k^\top \beta = 0 | y) = 0$ for a continuous posterior distribution, we can test $H_0^{(k)} : c_k^\top \beta = 0$ against $H_1^{(k)} : c_k^\top \beta \neq 0$ for K nonzero $p \times 1$ vectors c_1, \dots, c_K using a classical linear model, $y = X\beta + \eta, \eta \sim N_n(0_n, \sigma^2 V_y)$, where β is fixed but unknown (e.g., [Seber and Lee, 2003](#)). We compute $t_{\text{obs}}^{(k)} = \frac{c_k^\top \hat{\beta}}{\hat{\sigma} \sqrt{c_k^\top (X^\top V_y^{-1} X)^{-1} c_k}}$ for each c_k , where $\hat{\beta} = (X^\top V_y^{-1} X)^{-1} X^\top V_y^{-1} y$ and $(n-p)\hat{\sigma}^2 = (y - X\hat{\beta})^\top V_y^{-1} (y - X\hat{\beta})$ are generalized least squares estimates. We reject $H_0^{(k)}$ if the p-values $p_k = \mathbb{P}\left(T > |t_{\text{obs}}^{(k)}|\right)$, where $T \sim t_{n-p}$, are below a multiplicity adjusted threshold.

In contrast to assuming strict equality in the point null hypothesis, equivalence tests define a margin around the null value where the effect size is not considered to be practically different from the null value. Bayesian approaches based on this “region of practical equivalence” (ROPE) follow a similar logic and enable full probabilistic statements about the distribution of the parameter within the ROPE ([Kruschke and Liddell, 2018](#); [Makowski et al., 2019](#)). Here, we follow a similar approach by retaining the continuous conjugate prior for β and evaluating the posterior probabilities for the absolute standardized linear combinations between elements of β to exceed a threshold ϵ . Hence, for all $k = 1, \dots, K$ and any $\epsilon > 0$, we define

$$v_k(\epsilon) = \mathbb{P}\left(\frac{|c_k^\top \beta|}{\sigma \sqrt{c_k^\top M c_k}} > \epsilon \mid y\right). \quad (8)$$

We refer to these posterior probabilities as ϵ -difference probabilities, where ϵ represents a universal threshold or equivalence margin across all K linear combinations indicating the number of posterior standard deviation units that $|c_k^\top \beta|$ is away from 0. If $\beta^{(1)}, \dots, \beta^{(N)}$ and $\sigma^{(1)}, \dots, \sigma^{(N)}$ are N samples drawn from their respective posterior distributions, then we estimate (8) using

$$\hat{v}_k(\epsilon) = \frac{1}{N} \sum_{t=1}^N \mathbb{I}\left(\frac{|c_k^\top \beta^{(t)}|}{\sigma^{(t)} \sqrt{c_k^\top M c_k}} > \epsilon\right) \quad (9)$$

for any given ϵ . Adapting (2) to $\gamma = 0$ yields $\pi(\beta, \sigma^2 | y) = N(\beta | Mm, \sigma^2 M) \times \text{IG}(\sigma^2 | a, b)$, where $a = a_0 + \frac{n}{2}$, $b = b_0 + \frac{1}{2} (y^\top V_y^{-1} y + m_0^\top M_0 m_0 - m^\top M m)$, $M^{-1} = M_0^{-1} + X^\top V_y^{-1} X$ and $m = m_0 + X^\top V_y^{-1} y$. We draw exact posterior samples from the Normal-Gamma family. Specific domain applications can provide further information on possible constraints for ϵ and on defining a clinically significant difference between coefficients β_i and β_j , which, for example, could represent mean results for different treatment groups in a Bayesian Analysis Of Variance (ANOVA).

The classical p-values and the probabilities $\{v_k(\epsilon)\}_k$ defined in (8) have opposite interpretation: a small value of p_k suggests that $|c_k^\top \beta|$ is far from 0, while small $v_k(\epsilon)$ suggests that $|c_k^\top \beta|$ is likely to be close to 0. In fact, Bayesian inference with a flat prior on β amounts to using the classical

generalized least squares estimate $\widehat{\beta}$. Hence, with a specific prior, the p-values and ϵ -difference probabilities yield identical decisions on contrasts in the following sense.

Theorem 1. *Let $c_1, \dots, c_K \in \mathbb{R}^p$, $X \in \mathbb{R}^{n \times p}$, $y \in \mathbb{R}^n$ and $V_y \in \mathbb{R}^{n \times n}$ be fixed. Under the standard linear model $y \sim N_n(X\beta, \sigma^2 V_y)$, let p_k be the p-value to test the null hypothesis $H_0^{(k)} : c_k^\top \beta = 0$ against $H_1^{(k)} : c_k^\top \beta \neq 0$ for $k = 1, \dots, K$. Then, $p_k > p_{k'}$ if and only if $v_k(\epsilon) < v_{k'}(\epsilon)$ for all $k \neq k'$, where $v_k(\epsilon) = \mathbb{P} \left(\frac{|c_k^\top \beta|}{\sigma \sqrt{c_k^\top M c_k}} > \epsilon \mid y \right)$ under $\pi(\beta, \sigma^2) \propto \pi(\sigma^2)$.*

Proof. See Section S1.

Theorem 1 implies that the ascending order of the p-values associated with null hypotheses $H_0^{(k)} : c_k^\top \beta = 0$ with the two-sided alternative $H_1^{(k)} : c_k^\top \beta \neq 0$ is equivalent to the descending order of the Bayesian ϵ -difference probabilities. Since this result holds for all $\epsilon > 0$ and the classical procedure does not depend on ϵ , the Bayesian rankings are stable with respect to ϵ .

3.2. Extension to Spatial Random Effects. We consider (1), where each observation corresponds to one region. We let V_ϕ be known, while ρ can be either a fixed hyperparameter or a random variable with a prior density. Generalizing the ϵ -difference probabilities in the fixed effects model, we perform posterior inference on random variables $r_k(\epsilon) = \mathbb{I} \left(\frac{|c_k^\top \gamma_\star|}{\sigma \sqrt{c_k^\top M_\star c_k}} > \epsilon \right)$ for any given $\epsilon > 0$. For $k = 1 \dots, K$, we define

$$h_k(\epsilon; \rho) = \mathbb{P} \left(\frac{|c_k^\top \gamma_\star|}{\sigma \sqrt{c_k^\top M_\star c_k}} > \epsilon \mid y, \rho \right), \quad (10)$$

where $c_k \in \mathbb{R}^{n+p}$ is a contrast on $\gamma_\star = (\beta^\top, \gamma^\top)^\top$. If $c_k^\top \gamma_\star = a_k^\top \gamma$ for some $a_k \in \mathbb{R}^n$, then $h_k(\epsilon; \rho) = \mathbb{P} \left(\frac{|a_k^\top \phi|}{\sqrt{a_k^\top \text{Var}(\phi \mid y, \sigma^2, \rho) a_k}} > \epsilon \mid y, \rho \right)$ where $\text{Var}(\phi \mid y, \sigma^2, \rho)$ is given by (4).

In the context of detecting spatial disparities, consider K pairs of neighboring regions $L = \{(i, j) : i < j, i \sim j\}$, where $i \sim j$ means that the regions i and j are neighbors. If $c_{ij} \in \mathbb{R}^{n+p}$ and $a_{ij} \in \mathbb{R}^n$ are such that $c_{ij}^\top \gamma_\star = a_{ij}^\top \gamma = \gamma_i - \gamma_j$, then the corresponding ϵ -difference probability is $h_{ij}(\epsilon; \rho) = \mathbb{P} \left(\frac{|\phi_i - \phi_j|}{\sqrt{a_{ij}^\top \text{Var}(\phi \mid y, \sigma^2, \rho) a_{ij}}} > \epsilon \mid y, \rho \right)$. Here, ϵ represents the equivalence margin for the combined contribution from all latent health effects averaged within each area after adjusting for known risk factors in X . Using (1) and (2), we extend the insights obtained from Theorem 1 and show that the ranking of conditional posterior probabilities $h_1(\epsilon), \dots, h_K(\epsilon)$ is stable with respect to ϵ for any $\rho \in (0, 1)$.

Theorem 2. *Let $\pi(\gamma, \beta, \sigma^2) = N_n(\gamma \mid 0, \sigma^2 \rho V_\phi) \times N_p(\beta \mid M_0 m_0, \sigma^2 M_0) \times IG(\sigma^2 \mid a_{\sigma^2}, b_{\sigma^2})$ be the prior distribution for the model in (1). Let $c_1, \dots, c_K \in \mathbb{R}^{n+p}$ and $X \in \mathbb{R}^{n \times p}$ be fixed. Define $h_k(\epsilon; \rho) = \mathbb{P} \left(\frac{|c_k^\top \gamma_\star|}{\sigma \sqrt{c_k^\top M_\star c_k}} > \epsilon \mid y, \rho \right)$ for $k = 1, \dots, K$, where $\epsilon > 0$ and $\rho \in (0, 1)$. If there exists $\epsilon_\star > 0$ such that $h_k(\epsilon_\star; \rho) < h_{k'}(\epsilon_\star; \rho)$ for any $k \neq k'$, then $h_k(\epsilon; \rho) < h_{k'}(\epsilon; \rho)$.*

Proof. See Section S2.

If $\pi(\rho)$ denotes the prior for ρ , then the marginal posterior distribution of γ_\star is analytically inaccessible and we define the ϵ -difference probability for any $c_k \in \mathbb{R}^{(n+p) \times 1}$ as

$$v_k(\epsilon) = \mathbb{P} \left(\frac{|c_k^\top \gamma_\star|}{\sigma \sqrt{c_k^\top (X_\star^\top V_{y_\star}^{-1} X_\star)^{-1} c_k}} > \epsilon \mid y \right) = \int_0^1 h_k(\epsilon; \rho) \pi(\rho \mid y) d\rho. \quad (11)$$

Given posterior samples $\gamma_\star^{(1)}, \dots, \gamma_\star^{(N)}$ and $\rho^{(1)}, \dots, \rho^{(N)}$, we estimate (11) by

$$\widehat{v}_k(\epsilon) = \frac{1}{N} \sum_{t=1}^N \mathbb{I} \left(\frac{|c_k^\top \gamma_\star^{(t)}|}{\sigma^{(t)} \sqrt{c_k^\top \left(X_\star^\top \left(V_{y_\star}^{(t)} \right)^{-1} X_\star \right)^{-1} c_k}} > \epsilon \right), \quad (12)$$

where $V_{y_\star}^{(t)} = \begin{bmatrix} (1 - \rho^{(t)})I_n & 0 & 0 \\ 0 & M_0 & 0 \\ 0 & 0 & \rho^{(t)}V_\phi \end{bmatrix}$. Since $V_{y_\star}^{(t)}$ depends on the sampled value of $\rho^{(t)}$,

computing $\text{Var}(\gamma_\star \mid y, \sigma^2, \rho)$ for each posterior sample requires inverting an $(n + p) \times (n + p)$ matrix for each posterior sample, which can become cumbersome. When we are only interested in linear combinations of spatial effects γ , the computation of $\text{Var}(\phi \mid y, \sigma^2, \rho)$ is significantly accelerated by utilizing $\text{Var}(\phi \mid y, \sigma^2, \rho) = U \left(I_n + \frac{\rho}{1-\rho} D \right)^{-1} U^\top$ as an alternate expression for (5) in Algorithm S2, where U and D are defined in Section 2.2 with a flat prior on β .

The choice of $\pi(\rho)$ is crucial for efficiently sampling the posterior joint of $\{\beta, \gamma, \sigma^2, \rho\}$ using MCMC and computing (12). Non-informative priors, such as uniform distributions on $[0, 1]$, induce extreme posterior overfitting in overly parameterized models (Gelman, 2006; Simpson et al., 2017). Instead, we consider the class of penalized complexity (PC) priors introduced in Simpson et al. (2017) as a means to encourage model parsimony and construct priors imparting a better interpretation. We follow Riebler et al. (2016) by placing a PC prior on ρ , denoted by $\text{PC}(\rho \mid \lambda_\rho, V_\phi) \propto \lambda_\rho \exp(-\lambda_\rho d(\rho; V_\phi))$ for $0 \leq \rho \leq 1$, where $\lambda_\rho > 0$ is a fixed hyperparameter, $d(\rho; V_\phi) = \sqrt{2D_{KL}(p(y; \rho) \parallel q(y))}$ and $D_{KL}(p(y; \rho) \parallel q(y))$ is the Kullback-Leiber divergence between $p(y; \rho) = N_n(y \mid 0_n, \rho V_\phi + (1 - \rho)I_n)$ and the base model without structured variance $q(y) = N_n(y \mid 0_n, I_n)$. The hyperparameter λ_ρ is chosen such that $P(\rho \leq U) = a$ where U and a are constants. Riebler et al. (2016) present promising simulation results demonstrating the PC prior's ability to shrink towards the simpler models with only spatial or non-spatial error variance. When $\pi(\beta, \gamma, \sigma^2, \rho) = N_n(\gamma \mid 0, \sigma^2 \rho V_\phi) \times \text{IG}(\sigma^2 \mid a_{\sigma^2}, b_{\sigma^2}) \times \text{PC}(\rho \mid \lambda_\rho, V_\phi)$, Algorithm S1 provides Gibbs updates for $\{\beta, \gamma, \sigma^2\}$ and a Metropolis-Hastings update for ρ . We assess predictive fit using data replicates, where one instance of $y_{rep}^{(t)} \sim N_n(X\beta^{(t)} + \gamma^{(t)}, \sigma^{2(t)}(1 - \rho^{(t)})I_n)$ is sampled for each drawing of the posterior samples $\{\beta^{(t)}, \gamma^{(t)}, \sigma^{2(t)}, \rho^{(t)}\}$.

3.3. Difference Probabilities in Generalized Linear Mixed Models. The stability of rankings of conditional posterior probabilities is established in the previous sections using a normally distributed outcome. More generally, for generalized linear mixed models theoretical tractability is lost when the outcome follows a probability distribution from the exponential family with link function

$$g(\mathbb{E}(y_i | \beta, \gamma_i, \eta_i)) = x_i^T \beta + \gamma_i + \eta_i, \quad (13)$$

where x_i is $p \times 1$ consisting of values of covariates for the i -th observation, $i = 1, \dots, n$, $\gamma \sim N_n(\gamma | 0_n, \sigma^2 \rho V_\phi)$, and $\eta \sim N_n(0, \sigma^2(1 - \rho)I_n)$. The link function $g(\cdot)$ relates the mean result to covariates and random effects and is commonly chosen as the canonical link such that (13) is the natural parameter of the exponential family distribution of y_i .

We use posterior samples using MCMC to estimate difference probabilities of the form

$$\tau_k(\epsilon) = \mathbb{P} \left(\frac{|c_k^T \gamma_\star|}{\sqrt{\text{Var}(c_k^T \gamma_\star | y)}} > \epsilon \mid y \right), \quad (14)$$

where $\gamma_\star = (\beta^T, \gamma^T)^T$. The marginal posterior variance is estimated with the posterior samples by $\widehat{\text{Var}}(c_k^T \gamma_\star | y) = \frac{1}{T-1} \sum_{t=1}^T (c_k^T \gamma_\star - c_k^T \bar{\gamma}_\star)^2$ where $\bar{\gamma}_\star = \frac{1}{T} \sum_{t=1}^T \gamma_\star^{(t)}$. The order of τ_1, \dots, τ_K may still be stable with respect to choice of ϵ if the marginal posterior distribution of γ_\star resembles, for example, a multivariate normal or t distribution.

We note that this approach for non-Gaussian outcomes has a weakness for detecting spatial disparities: the choice of the link function $g(x)$ in (13) critically determines the interpretation of the difference probability. For example, if $g(x) = \log(x)$, the canonical link for a Poisson generalized linear model, then the differences $|\phi_i - \phi_j|$ must now be interpreted in terms of unscaled difference in adjusted log-relative risk, which may produce non-intuitive results. The difference probabilities corresponding to the boundaries in high-risk boundaries may be ranked lower than those of low-risk regions with similar geographic heterogeneity in observed rates. Depending on other risk factors, disparities in log-relative risk may be more frequent in low-risk regions with minimal differences in incidence rates. Difference probabilities based on transformations of the spatial residuals can offer one alternative resolution but may result in a different set of reported boundaries; we demonstrate this through a simulation example in Section 4.2, where the difference probability defined in (14) achieves superior classification performance when compared to a similar difference probability defined in terms of an adjusted incidence rate ratio. We otherwise focus our attention on the case of a normally distributed outcome and identity link function, applying equal weight to differences between rates in high-risk and low-risk regions.

3.4. A Bayesian FDR-Based Decision Rule. After computing the difference probability $\nu_k(\epsilon)$ for each linear combination of interest, we wish to account for multiple comparisons before constructing binary decisions because we are not operating under an automatically penalizing mixture model as in [Scott and Berger \(2006\)](#). We specifically safeguard against Type I errors by controlling the false discovery rate (FDR introduced in [Benjamini and Hochberg, 1995](#)), while retaining

power by minimizing the false negative rate (FNR). Thus, we define $\text{FDR} = \frac{\sum_{k=1}^K \mathbb{I}\left(\frac{|c_k^T \gamma_\star|}{\sigma \sqrt{c_k^T M_\star c_k}} \leq \epsilon\right) d_k}{\iota + \sum_{k=1}^K d_k}$,

$\text{FNR} = \frac{\sum_{k=1}^K \mathbb{I}\left(\frac{|c_k^T \gamma_\star|}{\sigma \sqrt{c_k^T M_\star c_k}} > \epsilon\right) (1-d_k)}{\iota + \sum_{k=1}^K (1-d_k)}$ where $\iota > 0$ is a small constant to avoid a zero denominator and $d_k \in \{0, 1\}$ represents our decision to declare $\frac{|c_k^T \gamma_\star|}{\sigma \sqrt{c_k^T M_\star c_k}} > \epsilon$. The FDR and FNR functions are random variables that have different interpretations in the two paradigms Müller et al. (2007).

Given a set of difference probabilities $\{v_1(\epsilon), \dots, v_K(\epsilon)\}$, we use the Bayesian FDR and FNR defined in Müller et al. (2004) as the posterior expectation

$$\overline{\text{FDR}}(t^\star, \epsilon) = \mathbb{E}[\text{FDR}(t^\star, \epsilon) | y] = \frac{\sum_{k=1}^K (1 - v_k(\epsilon)) \mathbb{I}(v_k(\epsilon) \geq t^\star)}{\sum_{k=1}^K \mathbb{I}(v_k(\epsilon) \geq t^\star)}, \quad (15)$$

$$\overline{\text{FNR}}(t^\star, \epsilon) = \mathbb{E}[\text{FNR}(t^\star, \epsilon) | y] = \frac{\sum_{k=1}^K v_k(\epsilon) \mathbb{I}(v_k(\epsilon) < t^\star)}{\sum_{k=1}^K \mathbb{I}(v_k(\epsilon) < t^\star)}. \quad (16)$$

Minimizing the $\overline{\text{FNR}}$ subject to $\overline{\text{FDR}} \leq \delta$ is achieved by decisions of the form $d_k = \mathbb{I}(v_k(\epsilon) \geq t^\star(\epsilon))$, where $t^\star(\epsilon) \in [0, 1]$ for all $\epsilon > 0$ is a threshold chosen as

$$t^\star(\epsilon) = \inf \left\{ t \in [0, 1] : \overline{\text{FDR}}(t, \epsilon) \leq \delta \right\}. \quad (17)$$

Bayesian and classical FDR compute posterior probabilities and p-values, respectively, which are used to rank the plausibility of each hypothesis before choosing a cut-off according to a decision rule. In general, the Bayesian FDR and its classical analogue are fundamentally different criterion that are not necessarily equivalent, and their respective control procedures may produce different sets of decisions. However, in the linear fixed effects model and the setting of Theorem 1, if the prior is noninformative on β in the Bayesian approach, then the order of the posterior probabilities is the reversed order of the p-values. In this case, the Bayesian and classical FDR control procedures differ only in the decision criterion; specific choice of the decision parameter δ in the Bayesian approach can afford decisions identical to many classical FDR control procedures.

For creating binary decisions, ϵ must be chosen to apply this Bayesian FDR control procedure. However, for any $\delta > 0$, if we set ϵ to be arbitrarily small and $t^\star = 0$, we would declare every decision positive as $d_k = 1$. On the other hand, if we set ϵ to be arbitrarily large and $t^\star = 1$, then we would declare every decision negative as $d_k = 0$. Both cases achieve $\overline{\text{FDR}} \leq \delta$, but do not induce meaningful statements about the data. This motivates a heuristic to choose ϵ at a reasonable value before applying the Bayesian FDR control procedure to create decisions.

3.5. Selecting an ϵ -difference threshold. In the absence of guidance on the choice of ϵ , we consider two general heuristics to select a reasonable value for ϵ , the first based on a loss function and the relationship between ϵ and our resulting actions. As ϵ increases, the event that a contrast exceeds ϵ standard deviations gains stronger meaning, but has a lower posterior probability. On the other hand, the event that a contrast is less than ϵ standard deviations becomes less precise but more

probable. This motivates the use of a loss function that is optimized with respect to ϵ by balancing the strength of our affirmative conclusions that a boundary is a disparity at the ϵ -difference level with the precision of our negative conclusions.

As a general heuristic, we appeal to the principle of maximum entropy, which suggests that, given a selection of possible posterior distributions, the posterior distribution that best represents our posterior knowledge is precisely the one with maximum entropy. The principle of maximum entropy (Jaynes, 1957) selects the maximum entropy distribution due to it being “maximally noncommittal” with respect to the amount of information we imbue the posterior with beyond the observed data. Under the model (1), choosing an extremely small or large difference threshold ϵ causes the posterior distribution of $r_k(\epsilon) = \mathbb{I}\left(\frac{|c_k^T \gamma_\star|}{\sigma \sqrt{c_k^T M_\star c_k}} > \epsilon\right)$ to collapse into a point mass at 1 or 0 respectively, which has minimal entropy. Maximizing the joint posterior entropy of $R = \{r_1(\epsilon), \dots, r_K(\epsilon)\}$ with respect to ϵ thus avoids obscuring the information that the data y provides on the true quantities of interest, $\left\{\frac{|c_1^T \gamma_\star|}{\sigma \sqrt{c_1^T M_\star c_1}}, \dots, \frac{|c_K^T \gamma_\star|}{\sigma \sqrt{c_K^T M_\star c_K}}\right\}$.

Shannon (1948) explains the Shannon entropy as an objective measure of the information or uncertainty of a probability distribution. Let I be a $K \times 1$ vector such that $I_k \in \{0, 1\}$ for all $k = 1, \dots, K$ and let $g(I) = \mathbb{P}(\cap_{k=1}^K r_k(\epsilon) = I_k \mid y)$. Since $r_k(\epsilon)$ is a binary random variable equal to 1 with posterior probability $v_k(\epsilon)$, the joint Shannon posterior entropy of R measured in nats is defined as $H(R) = -\sum_{I \in \{0,1\}^K} g(I) \log g(I)$. However, the joint entropy entails estimating 2^K probabilities and is computationally unfeasible even for moderate K .

Instead, we opt for maximizing the entropy of a uniformly chosen ϵ -difference indicator. For any $\epsilon > 0$, let J be a random variable with uniform probability mass on $\{1, \dots, K\}$ and $W_\epsilon = r_J(\epsilon)$. The conditional posterior entropy of W_ϵ given J is $H_J(W_\epsilon) = \frac{1}{K} \sum_{k=1}^K H(r_k(\epsilon))$. The sum of the individual entropies is related to the joint entropy by the sub-additivity property of the joint entropy (Shannon, 1948), which states that $H(R) \leq \sum_{k=1}^K H(r_k(\epsilon))$, where $H(r_k(\epsilon)) = -v_k(\epsilon) \log v_k(\epsilon) - (1 - v_k(\epsilon)) \log(1 - v_k(\epsilon))$. We obtain an optimal ϵ by maximizing the average of the individual entropies or, equivalently, minimizing

$$\text{LOSS}_{\text{CE}}(\epsilon) = \sum_{k=1}^K v_k(\epsilon) \log v_k(\epsilon) + (1 - v_k(\epsilon)) \log(1 - v_k(\epsilon)) , \quad (18)$$

which we refer to as the conditional entropy loss function. We denote the ϵ obtained from minimizing (18) as ϵ_{CE} . When $v_k(\epsilon)$ is unavailable in closed form, this loss function is estimated from the posterior samples using (9). For difference boundary analysis on a set L containing K pairs of neighboring regions and a corresponding set of difference probabilities, $\{v_{ij}(\epsilon)\}_{(i,j) \in L}$, the summation in (18) is over all pairs of neighboring regions, $(i, j) \in L$. In the special case of perfect spatial health equity where all difference probabilities are exactly equal for all ϵ , this procedure results in $v_{(i,j)}(\epsilon_{\text{CE}}) = 0.5$ for all boundaries (i, j) . Also, $v_k(\epsilon)$ is replaced with $h_k(\epsilon; \rho)$ defined in (10) when conditioning on a given $0 < \rho < 1$.

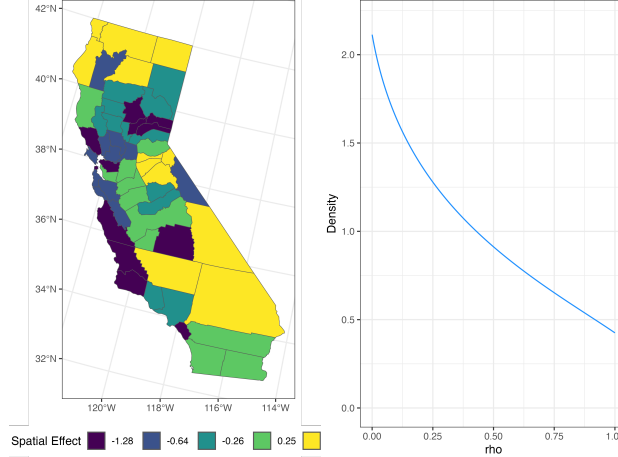


FIGURE 1. Left: simulated unscaled spatial effects ϕ . There are 90 difference boundaries separating counties with distinct spatial effects. Right: prior density of $\rho \sim \text{PC}(\lambda_\rho = 0.2)$.

As an alternative to optimizing (18), we can consider the number of positive decisions indicated by T . Fixing two quantities out of ϵ , δ and T determines the third, representing a three-way trade-off between protection against Type I errors, quantity, and quality in our positive results: δ indicates our tolerance for false positives; T is the quantity of positive results; and ϵ is our standard for a disparity, which reflects the quality of our decisions. If δ and T are fixed, then a valid choice of ϵ should belong to $A_\epsilon = \left\{ \epsilon > 0 : \overline{\text{FDR}}(t^*(\epsilon)) \leq \delta, \sum_{(i,j) \in L} d_{ij} \geq T \right\}$. This criterion can be more useful in policy settings aiming to identify rankings of the most egregious disparities, for example, the top fifty. However, this approach will always report T disparities, even if there are no significant differences between the regions. Finally, by fixing ϵ and T , δ implicitly equals the Bayesian FDR of the resulting decisions, although this does not represent active protection against Type I errors.

We conclude this section with a remark on the implications of the limiting cases discussed in Section 2.2. As ρ tends to 0, (6) indicates that boundary detection becomes meaningless because spatial effects converge to 0. As ρ tends to 1, σ^2 and γ also have limiting distributions described in (7), suggesting that the conditional variance of γ (in the definition of the ϵ -difference probability) or σ^2 will neither explode nor shrink toward 0 when ρ is near 1.

4. SIMULATION EXPERIMENTS

4.1. Simulation Comparison with ARDP-DAGAR. We compare difference boundary classification performance between our ϵ -difference approach and the areally-referenced Dirichlet process (ARDP) method introduced by Li et al. (2015) and expanded to the multivariate setting in Gao et al. (2023) in 100 simulated datasets on a map of the Californian counties.

To create a reference dataset, we first draw $z \sim N_n(0_n, \Sigma)$, where Σ is a exponential covariance kernel such that $\Sigma_{ij} = \exp(-d_{ij}/150)$ where d_{ij} is the Great Circle distance between the centroids

of regions i and j in kilometers. We divide the components z_1, \dots, z_n into quintiles and replace each component with the mean of the corresponding quintile. This neutral setup allows for a fair comparison between our proposed method and an existing Bayesian non-parametric approach. The resulting spatial effects ϕ are fixed across datasets and mapped in the left panel of Figure 1. Out of 139 total, there are 90 boundaries (i, j) where $\phi_i \neq \phi_j$, which we label as the true difference boundaries. We then generate 100 datasets $\{X^{(i)}, y^{(i)}\}$ by generating covariates $X^{(i)} = (1_n, x^{(i)})$, $x^{(i)} \sim N_n(0, I_n)$ and the response $y^{(i)} \sim N_n(X^{(i)}\beta + \gamma, \sigma^2(1 - \rho)I_n)$ with $\gamma = \sqrt{\sigma^2\rho}\phi$, $\rho = 0.95$, $\sigma^2 = 5$, and $\beta = (2, 5)^\top$.

For both methods, we compute difference probabilities over L , the set of all boundaries between Californian counties. For the ϵ -difference method, we employ the BYM2 model in (1) with the prior $\pi(\beta, \gamma, \sigma^2, \rho) = N_n(\gamma | 0_n, \sigma^2\rho V_\phi) \times \text{IG}(\sigma^2 | 0.001, 0.001) \times \text{Unif}(\rho | 0, 0.99)$. We use a spatial CAR prior with $V_\phi^{-1} = c(D_W - \alpha W)$ constructed using the adjacency relations of the Californian counties, $\alpha = 0.99$, and $c = 0.8352$ such that the geometric mean of the marginal prior variances of γ is equal to one. We choose $\lambda_\rho = 0.2$, corresponding to a prior belief that $\mathbb{P}(\rho \leq 0.5) \approx 0.67$ and truncate the support of ρ to the interval $[0, 0.99]$ to improve convergence. The density of $\text{PC}(\rho | \lambda_\rho = 0.2)$ is shown in Figure 1. For each dataset, we draw 20,000 posterior samples of $(\beta, \gamma, \rho, \sigma^2)$ after 40,000 burn-in samples using the Metropolis within Gibbs sampling algorithm detailed in Appendix S3, obtain ϵ_{CE} by minimizing (18), and estimate the difference probabilities $\{v_{ij}(\epsilon_{CE})\}_{(i,j) \in L}$ using (12).

The ARDP model builds spatial dependence through a Markov random field on a latent component and imbues the spatial effects with a probability distribution. Following the notation of Li et al. (2015), we write the ARDP model as

$$\begin{aligned} Y | \beta, \gamma, \sigma^2 &\sim N_n(X\beta + \gamma, \sigma^2 I_n), \quad \gamma \sim G_n, \quad G_n = \sum_{u_1, \dots, u_n} \pi_{u_1, \dots, u_n} \delta_{\zeta_{u_1}} \cdots \delta_{\zeta_{u_n}}; \\ \pi_{u_1, \dots, u_n} &= \mathbb{P} \left(\sum_{k=1}^{u_1-1} p_k < F^{(1)}(\phi_1) < \sum_{k=1}^{u_1} p_k, \dots, \sum_{k=1}^{u_n-1} p_k < F^{(n)}(\phi_n) < \sum_{k=1}^{u_n} p_k \right); \\ \zeta &\sim N_K(0, \sigma_s^2), \quad p_1 = V_1, \quad p_j = V_j \prod_{k < j} (1 - V_k), \quad V_j \stackrel{i.i.d.}{\sim} \text{Beta}(1, \alpha_V), \quad \phi \sim N_n(0, W_\phi), \end{aligned} \quad (19)$$

where $F^{(i)}(\cdot)$ is the CDF of the marginal component ϕ_i , u_1, \dots, u_n are indices sampled from $\{1, \dots, N\}$, and $\{p_1, \dots, p_K\}$ are the stick-breaking weights truncated to K clusters. The spatial components ϕ follow a directed acyclic graphical autoregression (DAGAR) model parameterized by $r \in (0, 1)$, a spatial autocorrelation parameter (Datta et al., 2019). The DAGAR model requires a specific ordering of the regions $\{1, \dots, n\}$, which we construct by sorting $\delta_1 < \delta_2 < \dots < \delta_n$ where $\delta_i = L_{i,1} - L_{i,2}$ and $(L_{i,1}, L_{i,2})$ are the coordinates of a Albers projection of the i th county's centroid. Denote $N(i)$ as the set of neighboring regions that precede i in the ordering and a_i is the number of regions in $N(i)$. Then, $W_\phi^{-1} = (I_n - B)^\top R_\phi (I_n - B)$, where $B_{ij} = 0$ if $j \notin N(i)$,

$B_{ij} = \frac{r}{1+(a_i-1)r^2}$ for $i = 2, \dots, n$ and $j \in N(i)$, and R_ϕ is a diagonal matrix with $(R_\phi)_{ii} = \frac{1+(a_i-1)r^2}{1-r^2}$ for $i = 1, \dots, n$.

We match the simulation settings in [Gao et al. \(2023\)](#) by setting the prior $\pi(\beta, \sigma^2, \sigma_s^2, r) = N_p(\beta | 0_p, 100^2 I_p) \times \text{IG}(\sigma^2 | 2, 0.1) \times \text{IG}(\sigma_s^2 | 2, 1) \times \text{Unif}(r | 0, 0.99)$ and fixing $\alpha_V = 1$. For each simulated data set, we draw $50,000 \times 4$ chains = 200,000 samples from the joint posterior $\pi(\beta, \gamma, \sigma^2, \sigma_s^2, \phi, r | y)$ after 50,000 burn-in samples per chain using the MCMC algorithm implemented in [Gao et al. \(2023\)](#). We use the posterior samples of γ to compute Monte Carlo estimates of the difference probabilities $w_{ij} = \mathbb{P}(\gamma_i \neq \gamma_j | y)$ for all neighboring pairs $(i, j) \in L$.

We also compare our results to spatial outlier detection with Local Moran’s I computed with “rook contiguity” weights based on the standardized residuals $z_i = e_i - \frac{1}{n} \sum_j e_j$ from an ordinary least squares regression of $y^{(i)}$ on $x^{(i)}$. We compute significance p-values for each region using 50,000 permutations and control the FDR at 0.15 with the classical method ([Benjamini and Hochberg, 1995](#)). If a region is significant after multiplicity adjustment, it is a high-low outlier if $z_i > 0$, $\sum_{j:i \sim j} z_j < 0$ or a low-high outlier if $z_i < 0$, $\sum_{j:i \sim j} z_j > 0$. We report (i, j) as a difference boundary if the region i is a high-low or low-high outlier and the region j is not significant or is not of the same type of outlier.

The difference probabilities $v_{ij}(\epsilon)$ and $w_{ij}(\epsilon)$ have equivalent interpretation: a higher difference probability indicates a stronger posterior belief that (i, j) is a true difference boundary. For $T = 1, \dots, 139$, we take the boundaries corresponding to the top T difference probabilities as the reported difference boundaries in each dataset and average sensitivity and specificity across datasets for each method to obtain the averaged receiver operating characteristic (ROC) curve in the top left panel of Figure 2. For all values of T , our proposed framework shows comparable performance to the nonparametric alternative. The area under the ROC curve (AUC) for the ϵ -difference method is 0.856, while the AUC for the ARDP-DAGAR method is 0.871. When $T = 90$, the ϵ -difference method has an averaged sensitivity of 0.828 and a specificity of 0.683, while the ARDP-DAGAR method has an averaged sensitivity of 0.832 and specificity of 0.691.

We apply the FDR control in Section 3.4 with tolerance $\delta = 0.3$ for each data set and both types of difference probabilities. The top difference probabilities from ARDP-DAGAR in the top middle panel of Figure 2 belong to a few datasets, resulting in a large variation in the number of reported disparities, as shown in the right panel of Figure 2. The ARDP-DAGAR produced 58.59 (SD = 29.71) disparities reported on average, an overall false discovery rate of 10.68%, and 6 out of 50 datasets with zero reported disparities. Boundary detection based on Local Moran’s I reported 11.87 (SD = 6.63) disparities per data set on average, an overall false discovery rate of 4.30%, and 10 datasets reporting no disparities. The ϵ -difference approach reported 19.54 (SD = 8.45) disparities on average, an overall false discovery rate of 0.92%, and zero data sets with no reported disparities. Therefore, our approach shows an attractive decrease in the probability of reporting global non-significance while minimizing the false discovery rate.

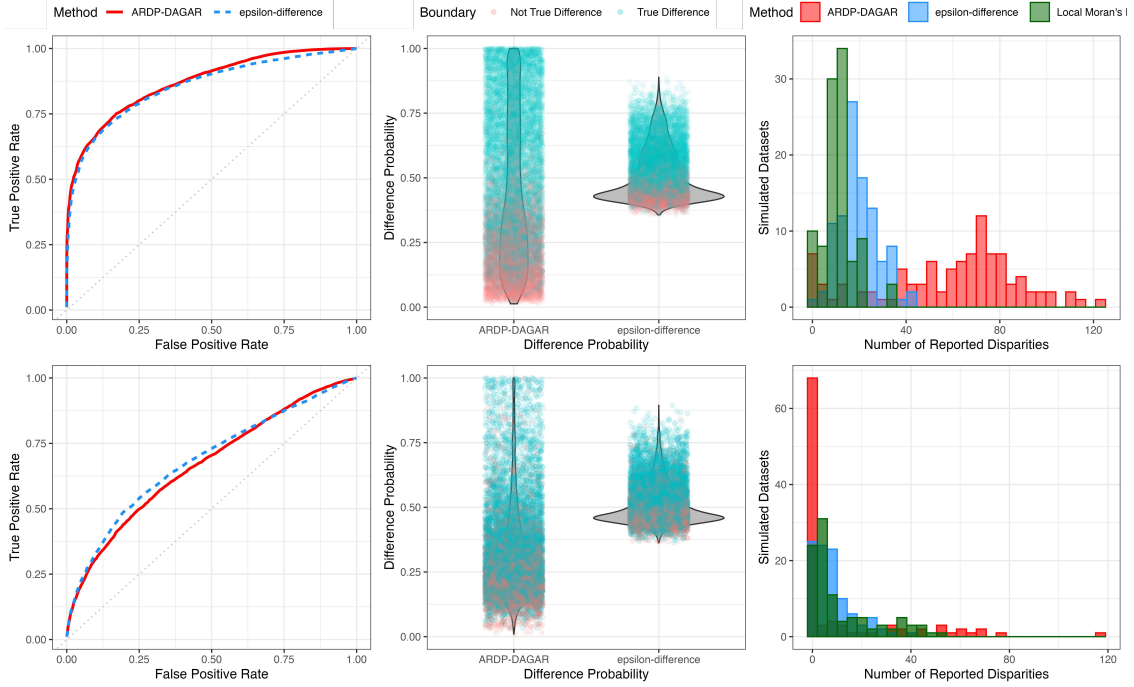


FIGURE 2. Classification performance of ϵ -difference method with CAR spatial kernel and ARDP-DAGAR method for data simulated with $\rho = 0.95$ (top panels) and $\rho = 0.7$ (bottom panels). Left: ROC curves showing true positive rate versus false positive rate colored by method across varying number of reported difference boundaries. Performance at each cutoff value is averaged across 100 simulated datasets. Middle: violin plots with of difference probabilities generated across each dataset and method. Difference probabilities corresponding to true simulated disparities are colored in blue. Right: histograms of the number of reported disparities in each dataset colored by method. The Bayesian FDR tolerance is set to $\delta = 0.3$ for the ARDP-DAGAR and ϵ -difference methods while the FDR-adjusted p-value significance threshold is set to 0.15 for boundary detection using Local Moran's I.

The performance of all three methods suffer greatly when the spatial signal-to-noise ratio decreases. We repeat the simulation runs with $\rho = 0.7$, and re-evaluate the aforementioned performance metrics in the bottom panels of Figure 2. The AUC for the ϵ -difference framework decreases to 0.684 and the AUC for the ARDP-DAGAR method decreases to 0.669. In both cases, our proposed framework on average achieves comparable classification performance to the ARDP-DAGAR approach and results in fewer datasets with zero reported disparities under identical constraints on the Bayesian FDR. Boundary detection using Local Moran's I resulted in a false discovery rate of 18.67%, while the ϵ -difference (8.97%) and ARDP-DAGAR (18.42%) methods provided greater control over the FDR.

Because of the discrete clustering property of Dirichlet process models, our approach performs better when the spatial residual surface is smooth and spans a wide range of values, while the ARDP-DAGAR method is more suitable when the spatial residuals fall into a small number of distinct levels. Our method may be more efficient for approximately normally distributed outcomes, in particular disease maps in which only one aggregated incidence or prevalence rate is recorded for each areal unit. Compared to spatial outlier detection methods such as those based on Local Indicators of Spatial Association, our approach offers full Bayesian model estimation and FDR control in the presence of non-spatial heterogeneity.

4.2. Simulated Count Outcome. We demonstrate our analysis framework for a simulated count outcome on a map of the $n = 58$ Californian counties. We simulate a latent risk factor $\gamma \sim N_n(0_n, \sigma^2 \rho W_\phi)$ and unstructured error $\eta \sim N_n(0_n, \sigma^2(1 - \rho)I_n)$ with $\sigma^2 = 2$, $\rho = 0.93$, and W_ϕ as an exponential covariance kernel such that $W_{\phi,ij} = \exp(-d_{ij}/50)$, where d_{ij} is the great circle distance between the centroids of county i and j in kilometers. We generate covariates $x_i = (1, x_{i1})^T$, $x_{i1} \sim N(2, 1)$ and exposure $E_i = \lceil H_i \rceil$, $H_i \sim \text{Unif}(10^4, 5 \cdot 10^4)$ for $i = 1, \dots, 58$. We simulate $y_i \sim \text{Poisson}(E_i \exp(x_i^T \beta + \gamma_i + \eta_i))$ with $\beta = (-5, 0.5)^T$. Here, we define the simulated rate as y_i/E_i and denote the boundary between county i and j as a true spatial disparity at the ϵ -difference level if $\frac{|\phi_i - \phi_j|}{a_{ij}^T W_\phi a_{ij}} > \epsilon$.

We analyze the simulated data using a Poisson likelihood with the link function in (13) as $g(y_i) = \log\left(\frac{y_i}{E_i}\right)$ and use the prior $\pi(\beta, \gamma, \eta, \sigma^2, \rho) \propto N_n(\gamma | 0_n, \sigma^2 \rho V_\phi) \times N_n(\eta | 0_n, \sigma^2(1 - \rho)I_n) \times \text{IG}(\sigma^2 | 0.1, 0.1) \times \text{PC}(\rho | 0.2)$. We place a CAR spatial prior on γ by fixing $V_\phi^{-1} = c(D_W - \alpha W)$ using the adjacency relations of the Californian counties, $\alpha = 0.99$, and $c = 0.8352$. Using Hamiltonian Monte Carlo implemented within the `rstan` package in R, we obtain $20,000 \times 4$ chains = 80,000 total posterior samples of $(\beta, \gamma, \sigma^2, \rho)$ after discarding 40,000 initial burn-in samples per chain. We consider L , the set of boundaries between two neighboring California counties, and use Monte Carlo estimates of $\{\tau_{ij}(\epsilon)\}_{(i,j) \in L}$ via (14) to minimize the conditional entropy loss and obtain the optimal difference threshold $\epsilon_{CE} = 0.738$. Of 139 total boundaries, 76 are a true disparity at the $\epsilon_{CE} = 0.738$ difference level.

We repeat the analysis with two alternative difference probability definitions: $\psi_{ij} = \mathbb{P}(|\phi_i - \phi_j| > \epsilon | y)$, based on the unstandardized log-rate difference, and $\theta_{ij} = \mathbb{P}(\exp(|\gamma_i - \gamma_j|) > \epsilon | y)$, based on the adjusted incidence rate ratio (IRR). For a fair comparison, we also define a pair (i, j) to be a true ψ -disparity on the ϵ -difference level if $|\phi_i - \phi_j| > \epsilon$ or a θ -disparity if $\exp(|\gamma_i - \gamma_j|) > \epsilon$. We minimize the conditional entropy loss function to obtain $\epsilon_1 = 0.465$ and $\epsilon_2 = 1.506$ for the ψ_{ij} and θ_{ij} difference thresholds, respectively.

Figure 3 shows maps of the simulated rates (left panel) and spatial residuals γ with the boundaries corresponding to the top 20 log-rate difference probabilities τ_{ij} (middle left) or IRR difference probabilities θ_{ij} (middle right). The two types of difference probabilities share 13 out of the top 20 difference boundaries and both types resulted in all pairwise difference probabilities being

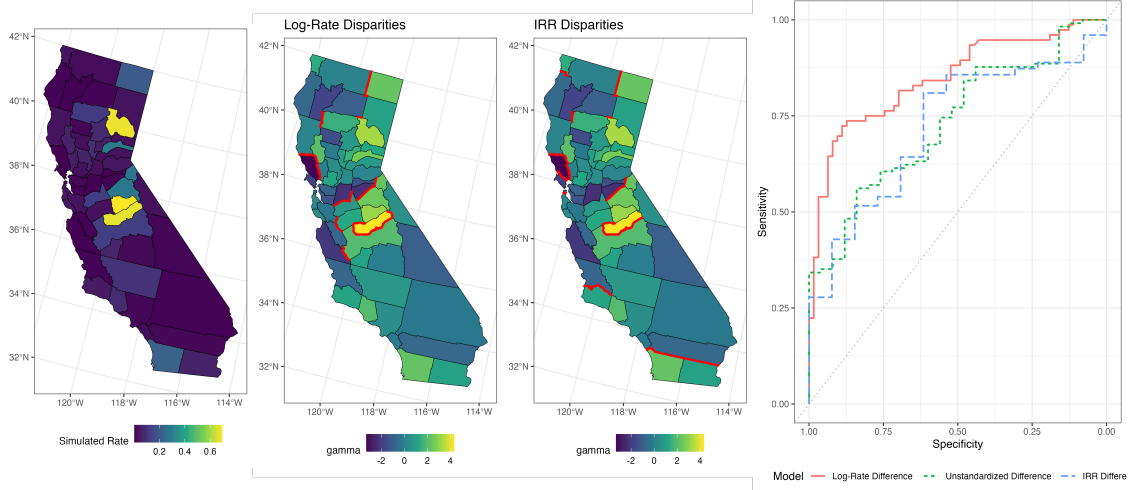


FIGURE 3. Boundary detection results for simulated count outcome on a California county map. From left to right: (1) Map of simulated rates y_i/E_i . (2) Map of simulated latent factors γ with (1) boundaries associated with top 20 $\epsilon_{CE} = 0.738$ standardized log-rate difference probabilities τ_{ij} and (3) boundaries associated with top 20 $\epsilon = 1.506$ IRR difference probabilities $\theta_{ij} = \mathbb{P}(\exp(|\phi_i - \phi_j|) > \epsilon | y)$. (4) ROC curves showing true positive rate versus true negative rate across varying cutoff values using τ_{ij} difference probabilities (red; AUC = 0.847), $\psi_{ij} = \mathbb{P}(|\phi_i - \phi_j| > \epsilon | y)$ difference probabilities (green; AUC = 0.733), and $\theta_{ij} = \mathbb{P}(\exp(|\gamma_i - \gamma_j|) > \epsilon | y)$ difference probabilities (blue; AUC = 0.723).

below 0.70. We evaluate the overall classification performance of the difference probabilities $\{v_{ij}(\epsilon)\}_{(i,j) \in L}$ in detecting spatial disparities and obtain a favorable classification performance shown by the ROC curve (AUC = 0.847) in the rightmost panel of Figure 3. We obtain an AUC value of 0.733 when using ψ_{ij} difference probabilities to detect ψ -disparities and an AUC value of 0.723 when using θ_{ij} difference probabilities to detect θ -disparities.

To evaluate rank stability, we compute the Spearman correlation between $\{\tau_{ij}(\frac{1}{3}\epsilon_{CE})\}_{(i,j) \in L_S}$ and $\{\tau_{ij}(3\epsilon_{CE})\}_{(i,j) \in L_S}$ as $r_s = 0.903$, which we consider as a rank stability score. The rank stability score using the unstandardized difference in ψ_{ij} is 0.825, indicating that the proposed difference probability formulation τ_{ij} in (14) offers improved classification performance and robustness in the rankings of the top difference probabilities under this simulation example.

5. APPLICATION

We analyze publicly available health data from the Institute of Health Metrics and Evaluation (IHME) on age-standardized county-level estimates of mortality rates in tracheal, bronchus, and lung cancer in 2014 (Mokdad et al., 2017). We adjust for multiple risk factors by incorporating county-level estimates of smoking prevalence in both sexes in 2012, physical inactivity in 2014,

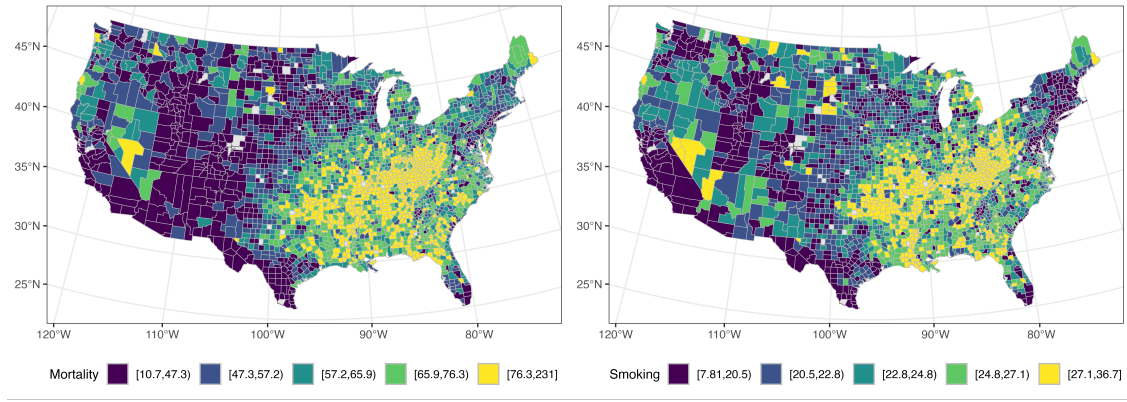


FIGURE 4. Left: map of county-level age-standardized mortality rate estimates for lung cancer in 2014, colored by quintile. Right: map of county-level total smoking prevalence estimates in 2012, colored by quintile.

percentage of residents 18 years or older without health insurance from 2012 to 2016, unemployment rate percentile (0-1.0) in 2014, overall social vulnerability index (SVI) percentile in 2014, adult diabetes prevalence in 2014, and adult obesity prevalence in 2014. Smoking prevalence was originally derived using data from the Behavioral Risk Factor Surveillance System in [Dwyer-Lindgren et al. \(2014\)](#), while data for all other risk factors was downloaded from the publicly available US Diabetes Surveillance System ([Centers for Disease Control and Prevention](#)). Previous work in [Shreves et al. \(2023\)](#) indicates that lung cancer mortality rates exhibit spatial autocorrelation that is not completely accounted for by smoking prevalence.

For our study region, we subset into $n = 3,017$ contiguous US counties with available estimates for smoking prevalence and lung cancer mortality rates with the aim of detecting disparities corresponding to county boundaries. Although we drop counties with missing data for the sake of simplicity in this application, one can refer to [Rubin \(1976\)](#) for an introduction to Bayesian approaches to missing data or [Ma and Chen \(2018\)](#) for a modern overview. For simplicity, we drop these counties from our study region as the remaining counties form a contiguous region. The cancer mortality rate and estimates of total smoking prevalence for the final study region are shown in Figure 4. High-risk regions can be clearly identified, most notably in the East South Central states, and our analysis aims to identify local health inequity at the county level.

To assess spatial autocorrelation, we fit an ordinary least squares linear model with the aforementioned risk factors as predictors of lung cancer mortality before computing Moran’s $I = 0.397$ and Geary’s $C = 0.586$ using the residuals ([Banerjee et al., 2015](#)). Both statistics were significant with 10,000 random permutations (p-value = $1/10,001$), suggesting that spatial autocorrelation is not fully captured by linearly regressing mortality rates on smoking prevalence.

We employ (1) such that $y | \beta, \gamma, \sigma^2, \rho \sim N_n(X\beta + \gamma, \sigma^2(1 - \rho)I_n)$ where β is the vector of regression coefficients with an intercept. Similarly to the simulation examples, we place a CAR

prior on ϕ by setting $V_\phi^{-1} = c(D_W - \alpha W)$, where the neighbor and adjacency matrices are computed using the subset of US counties, $\alpha = 0.99$, and $c = 0.3762$. We treat ρ as an unknown parameter and specify the joint prior as $\pi(\beta, \gamma, \sigma^2, \rho) = N_n(\gamma | 0, \sigma^2 \rho V_\phi) \times \text{IG}(\sigma^2 | a_{\sigma^2}, b_{\sigma^2}) \times \text{PC}(\rho | \lambda_\rho)$, where $a_{\sigma^2} = 0.1$ and $b_{\sigma^2} = 0.1$. Although the set of regions here differs slightly from the simulation example, we also set $\lambda_\rho = 0.0335$ as it approximately satisfies $\mathbb{P}(\rho \leq 0.5) = \frac{2}{3}$.

After 10,000 burn-in samples, we draw 30,000 samples from the posterior of $\{\beta, \gamma, \sigma^2, \rho\}$ using Algorithm S2. Table 1 presents 95% credible intervals for the nonspatial effect parameters, indicating that smoking, SVI percentile, physical inactivity, and uninsured rate are significant predictors of lung cancer mortality. The credible interval of ρ suggests that we are able to learn effectively about ρ , and the CAR spatial model explains most of the variance in the data.

| Parameter | Description | Posterior Mean | 95% Credible Interval |
|------------|--------------------------------|----------------|-----------------------|
| β_0 | Intercept | 9.56 | (4.828, 14.223) |
| β_1 | Smoking prevalence (%) | 1.90 | (1.754, 2.052) |
| β_2 | Unemployment percentile | 1.85 | (-0.473, 4.174) |
| β_3 | SVI percentile | 5.70 | (2.755, 8.68) |
| β_4 | Physically inactive (%) | 0.35 | (0.202, 0.49) |
| β_5 | Uninsured (%) | -0.60 | (-0.746, -0.451) |
| β_6 | Diabetes prevalence (%) | 0.18 | (-0.137, 0.506) |
| β_7 | Obesity prevalence (%) | 0.06 | (-0.08, 0.2) |
| σ^2 | Total variance | 108.25 | (95.927, 123.349) |
| ρ | Spatial proportion of variance | 0.78 | (0.692, 0.861) |

TABLE 1. Posterior summaries of non-spatial effect parameters in analysis of US county-level lung cancer mortality rates.

We detect spatial disparities using the ϵ -difference framework in Section 3. For this dataset, we denote the set of all $K = 8,793$ pairs of neighboring counties as $L = \{(i, j) : i < j, i \sim j\}$ and ϵ -difference probabilities of the form $v_{ij}(\epsilon) = \mathbb{P}\left(\frac{|\phi_i - \phi_j|}{\sqrt{a_{ij}^T \text{Var}(\phi | y, \sigma^2, \rho) a_{ij}}} > \epsilon \mid y\right)$ for all $(i, j) \in L$. We select the difference threshold ϵ by minimizing the conditional entropy loss in (18), which yields $\epsilon_{CE} = 0.922$. For this analysis, we set a maximum allowable Bayesian FDR of $\delta = 0.05$, compute $t^* = 0.884$ using (17) and report 722 county boundaries exhibiting spatial disparities.

The posterior predictive means and detected disparities are mapped in Figure 5. The reported disparities are mainly in relatively high risk states (KY, GA, TN, WV, MS, MO, VA), where several county mortality rate estimates are in the upper quintile with a wide range, suggesting prevalence of health inequities on the local county scale. These disparities between neighboring counties may be caused by a combination of local differences between counties' health policies or other latent determinants of health. Although our model assumes a global effect from each risk

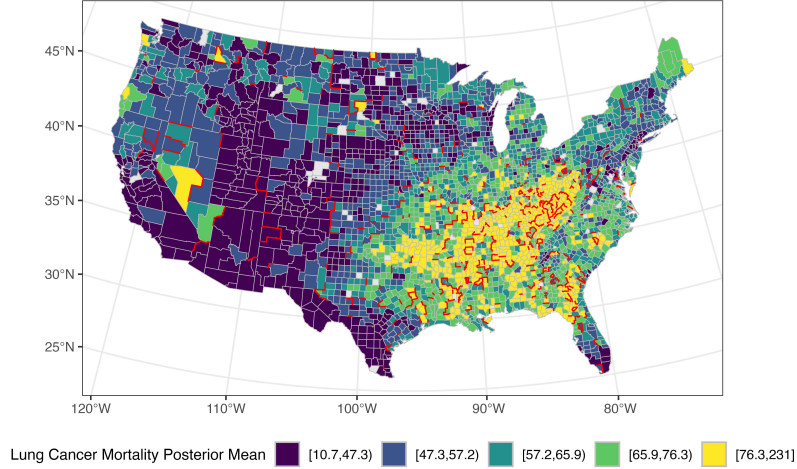


FIGURE 5. Map of posterior predictive means of lung cancer mortality rates. Red lines correspond to disparities between neighboring counties with difference threshold $\epsilon_{CE} = 0.922$ and Bayesian FDR tolerance $\delta = 0.05$.

factor, previous analysis by [Dong et al. \(2022\)](#) suggests that the association of risk factors such as obesity/diabetes prevalence and physical inactivity with cancer mortality may vary by geographical region. The complete list of 722 detected difference boundaries ranked by their corresponding difference probabilities is available in Table [S2](#).

6. DISCUSSION

Our ϵ -based difference boundary detection is considerably simpler to implement and interpret than Bayesian nonparametric approaches ([Gao et al., 2023](#); [Li et al., 2015](#)). We are able to stabilize the difference probabilities with respect to ϵ , which allows public health officials to report, say, the top 50 disparities between neighboring counties in a robust way. We could also define a difference boundary based on the posterior predictive distribution or the posterior distribution of the total residuals ($\gamma + \eta$) rather than the spatial random effects to identify transitions in the original health outcome or deviations from the explanatory model. We provide some insights in Section [S4](#) and establish stabilized rankings for the exact conjugate model. This may be preferred in public health practice because of its interpretation in terms of the health outcome itself, but such differences will conflate disparities attributed to space with nonspatial explanatory variables or risk factors. Future areas of investigations will include the impact of spatial confounding on ϵ -based boundary detection, and extending our framework to multivariate modeling with dependent outcomes. For computational efficiency, we will also develop Bayesian predictive stacking (as developed in [Pan et al., 2025](#); [Zhang et al., in press](#), for Gaussian process models) to avoid MCMC iterations and achieve exact Bayesian boundary detection by stacking over conjugate Bayesian models corresponding to different values of ρ .

SUPPLEMENTARY MATERIALS

Supplementary materials contain derivation of rank-stability results, sampling algorithm details, formulation of an ϵ -difference probability on the modeled response level, simulation analyses of classification performance sensitivity to the choice of ϵ and uncertainty in ρ , and the full list of spatial disparities in the data analysis. Computer programs that reproduce results in this manuscript are available at https://github.com/Ky-Wu/bayesian_spatial_health_disparities.

Algorithms S2 and S1 are executed in R using RcppArmadillo, the ARDP-DAGAR approach is executed using rjags, and MCMC sampling for the BYM2 Poisson model in Section 4.2 is performed using rstan. This work used computational and storage services associated with the Hoffman2 Shared Cluster provided by the UCLA Office of Advanced Research Computing’s Research Technology Group.

REFERENCES

- L. Aiello and S. Banerjee. Detecting Spatial Health Disparities Using Disease Maps. <https://arxiv.org/abs/2309.02086v2>, 2025.
- S. Banerjee, B. P. Carlin, and A. E. Gelfand. *Hierarchical Modeling and Analysis for Spatial Data*. Number 135 in Monographs on Statistics and Applied Probability. CRC Press, Taylor & Francis Group, Boca Raton, second edition, 2015. ISBN 978-1-4398-1917-3.
- G. E. Barboza-Salerno, S. Duhaney, B. Liebhard, and K. Schockley-McCarthy. Pushing the boundary of child well-being: A spatial examination of child mortality in transition zones of extreme economic inequality and material hardship. *PLOS One*, 20(8):e0330449, Aug. 2025. ISSN 1932-6203. doi: 10.1371/journal.pone.0330449.
- Y. Benjamini and Y. Hochberg. Controlling the False Discovery Rate: A Practical and Powerful Approach to Multiple Testing. *Journal of the Royal Statistical Society: Series B (Methodological)*, 57(1):289–300, 1995. ISSN 2517-6161. doi: 10.1111/j.2517-6161.1995.tb02031.x.
- J. Besag, J. York, and A. Mollié. Bayesian image restoration, with two applications in spatial statistics. *Annals of the Institute of Statistical Mathematics*, 43(1):1–20, Mar. 1991. ISSN 1572-9052. doi: 10.1007/BF00116466.
- D. Catelan and A. Biggeri. Multiple testing in disease mapping and descriptive epidemiology. *Geospatial Health*, 4(2):219–229, May 2010. ISSN 1970-7096. doi: 10.4081/gh.2010.202.
- Centers for Disease Control and Prevention. US Diabetes Surveillance System. <https://gis.cdc.gov/grasp/diabetes/diabetesatlas-analysis.html>.
- G. Copeland. The role of public health and how boundary analysis can provide a tool for public health investigations: The public health perspective. *Spatial and Spatio-temporal Epidemiology*, 1(4):201–205, Dec. 2010. ISSN 1877-5845. doi: 10.1016/j.sste.2010.09.002.
- F. Corpas-Burgos and M. A. Martinez-Beneito. On the use of adaptive spatial weight matrices from disease mapping multivariate analyses. *Stochastic Environmental Research and Risk Assessment*,

- 34:531–544, 2020.
- A. Datta, S. Banerjee, J. S. Hodges, and L. Gao. Spatial disease mapping using directed acyclic graph auto-regressive (DAGAR) models. *Bayesian analysis*, 14(4):1221, 2019.
- W. Dong, W. P. Bensken, U. Kim, J. Rose, Q. Fan, N. K. Schiltz, N. A. Berger, and S. M. Koroukian. Variation in and Factors Associated With US County-Level Cancer Mortality, 2008-2019. *JAMA Network Open*, 5(9):e2230925, Sept. 2022. ISSN 2574-3805. doi: 10.1001/jamanetworkopen.2022.30925.
- L. Dwyer-Lindgren, A. H. Mokdad, T. Srebotnjak, A. D. Flaxman, G. M. Hansen, and C. J. Murray. Cigarette smoking prevalence in US counties: 1996-2012. *Population Health Metrics*, 12(1):5, Mar. 2014. ISSN 1478-7954. doi: 10.1186/1478-7954-12-5.
- M. C. Fitzpatrick, E. L. Preisser, A. Porter, J. Elkinton, L. A. Waller, B. P. Carlin, and A. M. Ellison. Ecological boundary detection using bayesian areal wombling. *Ecology*, 91(12):3448–3455, 2010. doi: <https://doi.org/10.1890/10-0807.1>. URL <https://esajournals.onlinelibrary.wiley.com/doi/abs/10.1890/10-0807.1>.
- L. Gao, S. Banerjee, and B. Ritz. Spatial Difference Boundary Detection for Multiple Outcomes Using Bayesian Disease Mapping. *Biostatistics*, 24(4):922–944, Oct. 2023. ISSN 1465-4644. doi: 10.1093/biostatistics/kxac013.
- A. Gelman. Prior distributions for variance parameters in hierarchical models (comment on article by Browne and Draper). *Bayesian Analysis*, 1(3):515–534, Sept. 2006. ISSN 1936-0975, 1931-6690. doi: 10.1214/06-BA117A.
- M. E. Glickman, S. R. Rao, and M. R. Schultz. False discovery rate control is a recommended alternative to Bonferroni-type adjustments in health studies. *Journal of Clinical Epidemiology*, 67(8):850–857, Aug. 2014. ISSN 0895-4356. doi: 10.1016/j.jclinepi.2014.03.012.
- T. Hanson, S. Banerjee, P. Li, and A. McBean. Spatial boundary detection for areal counts. In *Nonparametric Bayesian Inference in Biostatistics*, pages 377–399. Springer, 2015.
- G. M. Jacquez. Geographic boundary analysis in spatial and spatio-temporal epidemiology: Perspective and prospects. *Spatial and Spatio-temporal Epidemiology*, 1(4):207–218, Dec. 2010. ISSN 1877-5845. doi: 10.1016/j.sste.2010.09.003.
- G. M. Jacquez and D. A. Greiling. Geographic boundaries in breast, lung and colorectal cancers in relation to exposure to air toxics in long island, new york. *International Journal of Health Geographics*, 2(1):1–22, 2003a. b.
- G. M. Jacquez and D. A. Greiling. Local clustering in breast, lung and colorectal cancer in long island, new york. *International Journal of Health Geographics*, 2(1):1–12, 2003b. a.
- J. S. Jagai, L. C. Messer, K. M. Rappazzo, C. L. Gray, S. C. Grabich, and D. T. Lobdell. County-level cumulative environmental quality associated with cancer incidence. *Cancer*, 123(15):2901–2908, 2017.
- E. T. Jaynes. Information Theory and Statistical Mechanics. *Physical Review*, 106(4):620–630, May 1957. ISSN 0031-899X. doi: 10.1103/PhysRev.106.620.

- J. K. Kruschke and T. M. Liddell. The Bayesian New Statistics: Hypothesis testing, estimation, meta-analysis, and power analysis from a Bayesian perspective. *Psychonomic Bulletin & Review*, 25(1):178–206, Feb. 2018. ISSN 1069-9384, 1531-5320. doi: 10.3758/s13423-016-1221-4.
- A. B. Lawson. *Statistical methods in spatial epidemiology*. John Wiley & Sons, 2013.
- B. Lawson, Andrew, S. Banerjee, R. Haining, and D. Ugarte, Maria. *Handbook of Spatial Epidemiology*. CRC press, Boca Raton, FL, 2016.
- D. Lee and R. Mitchell. Boundary detection in disease mapping studies. *Biostatistics*, 13(3): 415–426, July 2012. ISSN 1465-4644. doi: 10.1093/biostatistics/kxr036.
- P. Li, S. Banerjee, and A. M. McBean. Mining boundary effects in areally referenced spatial data using the bayesian information criterion. *Geoinformatica*, 15(3):435–454, 2011.
- P. Li, S. Banerjee, B. P. Carlin, and A. M. McBean. Bayesian areal wombling using false discovery rates. *Statistics and its Interface*, 5(2):149–158, 2012.
- P. Li, S. Banerjee, T. A. Hanson, and A. M. McBean. Bayesian models for detecting difference boundaries in areal data. *Statistica Sinica*, 25(1):385, 2015.
- H. Lu and B. P. Carlin. Bayesian areal wombling for geographical boundary analysis. *Geographical Analysis*, 37(3):265–285, 2005.
- H. Lu, C. S. Reilly, S. Banerjee, and B. P. Carlin. Bayesian areal wombling via adjacency modeling. *Environmental and ecological statistics*, 14:433–452, 2007.
- H. Ma and B. P. Carlin. Bayesian multivariate areal wombling for multiple disease boundary analysis. *Bayesian Analysis*, 2(2):281–302, 2007.
- H. Ma, B. P. Carlin, and S. Banerjee. Hierarchical and joint site-edge methods for medicare hospice service region boundary analysis. *Biometrics*, 66(2):355–364, 2010.
- Z. Ma and G. Chen. Bayesian methods for dealing with missing data problems. *Journal of the Korean Statistical Society*, 47(3):297–313, Sept. 2018. ISSN 2005-2863. doi: 10.1016/j.jkss.2018.03.002.
- D. Makowski, M. S. Ben-Shachar, S. H. A. Chen, and D. Lüdtke. Indices of Effect Existence and Significance in the Bayesian Framework. 10, Dec. 2019. doi: 10.3389/fpsyg.2019.02767.
- A. H. Mokdad, L. Dwyer-Lindgren, C. Fitzmaurice, R. W. Stubbs, A. Bertozzi-Villa, C. Morozoff, R. Charara, C. Allen, M. Naghavi, and C. J. L. Murray. Trends and Patterns of Disparities in Cancer Mortality Among US Counties, 1980-2014. *JAMA*, 317(4):388–406, Jan. 2017. ISSN 0098-7484. doi: 10.1001/jama.2016.20324.
- P. Müller, G. Parmigiani, C. Robert, and J. Rousseau. Optimal Sample Size for Multiple Testing. *Journal of the American Statistical Association*, 99(468):990–1001, Dec. 2004. ISSN 0162-1459. doi: 10.1198/016214504000001646.
- P. Müller, G. Parmigiani, and K. Rice. FDR and Bayesian Multiple Comparisons Rules. In *Bayesian Statistics 8: Proceedings of the Eighth Valencia International Meeting June 2–6, 2006*. Oxford University Press, July 2007. ISBN 978-0-19-921465-5. doi: 10.1093/oso/9780199214655.003.0014.

- S. Pan, L. Zhang, J. R. Bradley, and S. Banerjee. Bayesian inference for spatial-temporal non-Gaussian data using predictive stacking. 2025. URL <https://arxiv.org/abs/2406.04655>.
- J. S. Rao. *Statistical Methods in Health Disparity Research*. Chapman & Hall/CRC, Boca Raton, FL, 2023.
- A. Riebler, S. H. Sørbye, D. Simpson, and H. Rue. An intuitive Bayesian spatial model for disease mapping that accounts for scaling. *Statistical Methods in Medical Research*, 25(4):1145–1165, Aug. 2016. ISSN 0962-2802. doi: 10.1177/0962280216660421.
- F. Rodriguez, J. Hu, K. Kershaw, K. G. Hastings, L. López, M. R. Cullen, R. A. Harrington, and L. P. Palaniappan. County-Level Hispanic Ethnic Density and Cardiovascular Disease Mortality. *Journal of the American Heart Association*, 7(19):e009107, 2018.
- D. B. Rubin. Inference and missing data. *Biometrika*, 63(3):581–592, Dec. 1976. ISSN 0006-3444. doi: 10.1093/biomet/63.3.581.
- J. G. Scott and J. O. Berger. An exploration of aspects of Bayesian multiple testing. *Journal of Statistical Planning and Inference*, 136(7):2144–2162, July 2006. ISSN 0378-3758. doi: 10.1016/j.jspi.2005.08.031.
- G. A. Seber and A. J. Lee. Hypothesis Testing. In *Linear Regression Analysis*, chapter 4, pages 97–118. John Wiley & Sons, Ltd, 2003. ISBN 978-0-471-72219-9. doi: 10.1002/9780471722199.ch4.
- C. E. Shannon. A Mathematical Theory of Communication. *Bell System Technical Journal*, 27(3): 379–423, July 1948. ISSN 00058580. doi: 10.1002/j.1538-7305.1948.tb01338.x.
- A. H. Shreves, I. D. Buller, E. Chase, H. Creutzfeldt, J. A. Fisher, B. I. Graubard, R. N. Hoover, D. T. Silverman, S. S. Devesa, and R. R. Jones. Geographic Patterns in U.S. Lung Cancer Mortality and Cigarette Smoking. *Cancer Epidemiology, Biomarkers & Prevention*, 32(2):193–201, Feb. 2023. ISSN 1055-9965. doi: 10.1158/1055-9965.EPI-22-0253.
- D. Simpson, H. Rue, A. Riebler, T. G. Martins, and S. H. Sørbye. Penalising Model Component Complexity: A Principled, Practical Approach to Constructing Priors. *Statistical Science*, 32(1): 1–28, 2017. ISSN 0883-4237.
- T. Slack, C. A. Myers, C. K. Martin, and S. B. Heymsfield. The geographic concentration of us adult obesity prevalence and associated social, economic, and environmental factors. *Obesity*, 22(3):868–874, Mar. 2014. ISSN 1930-7381, 1930-739X. doi: 10.1002/oby.20502.
- W. S. Slutske, K. L. Conner, J. A. Kirsch, S. S. Smith, T. M. Piasecki, A. L. Johnson, D. E. McCarthy, P. Nez Henderson, and M. C. Fiore. Explaining COVID-19 related mortality disparities in American Indians and Alaska Natives. *Scientific Reports*, 13(1):20974, Nov. 2023. ISSN 2045-2322. doi: 10.1038/s41598-023-48260-9.
- W. Sun, B. J. Reich, T. T. Cai, M. Guindani, and A. Schwartzman. False Discovery Control in Large-Scale Spatial Multiple Testing. *Journal of the Royal Statistical Society. Series B, Statistical methodology*, 77(1):59–83, Jan. 2015. ISSN 1369-7412. doi: 10.1111/rssb.12064.

- W. Tansey, O. Koyejo, R. A. Poldrack, and J. G. Scott. False Discovery Rate Smoothing. *Journal of the American Statistical Association*, 113(523):1156–1171, July 2018. ISSN 0162-1459. doi: 10.1080/01621459.2017.1319838.
- N. Tian, P. Goovaerts, F. B. Zhan, and J. G. Wilson. Identification of racial disparities in breast cancer mortality: Does scale matter? *International Journal of Health Geographics*, 9(1):35, July 2010. ISSN 1476-072X. doi: 10.1186/1476-072X-9-35.
- M. Ventrucchi, E. M. Scott, and D. Cocchi. Multiple testing on standardized mortality ratios: A Bayesian hierarchical model for FDR estimation. *Biostatistics*, 12(1):51–67, Jan. 2011. ISSN 1465-4644. doi: 10.1093/biostatistics/kxq040.
- L. Waller and B. Carlin. Disease mapping. In A. E. Gelfand, P. Diggle, P. Guttorp, and M. Fuentes, editors, *Handbook Of Spatial Statistics*, page 217–243. CRC Press, Boca Raton, FL, 2010.
- L. A. Waller and C. A. Gotway. *Applied spatial statistics for public health data*, volume 368. John Wiley & Sons, 2004.
- L. Zhang, W. Tang, and S. Banerjee. Bayesian geostatistics using predictive stacking. *Journal of the American Statistical Association*, pages 1–19, in press. doi: 10.1080/01621459.2025.2566449. URL <https://doi.org/10.1080/01621459.2025.2566449>.

SUPPLEMENTARY MATERIAL FOR ASSESSING SPATIAL DISPARITIES: A BAYESIAN LINEAR REGRESSION APPROACH

KYLE LIN WU AND SUDIPTO BANERJEE

S1. PROOF OF THEOREM 1

Under the standard linear model described in Theorem 1, the p-values, $p_k = \mathbb{P}\left(t > |t_{\text{obs}}^{(k)}|\right)$, are characterized by a common t-distribution CDF evaluated at the observed t-statistics. As CDFs are monotonic functions, $p_k > p_{k'}$ if and only if $|t_{\text{obs}}^{(k)}| < |t_{\text{obs}}^{(k')}|$. Next, it is well known that when $\pi(\beta, \sigma^2) \propto \pi(\sigma^2)$, then $\beta | y, \sigma^2 \sim N\left(\widehat{\beta}, \sigma^2(X^T V_y^{-1} X)^{-1}\right)$, where $\widehat{\beta} = (X^T V_y^{-1} X)^{-1} X^T V_y^{-1} y$ is the generalized least-squares estimate. We have that for any $\epsilon > 0$, $\sigma^2 > 0$,

$$\begin{aligned} \mathbb{P}\left(\frac{|c_k^T \beta|}{\sigma \sqrt{c_k^T M c_k}} > \epsilon \mid y, \sigma^2\right) &= 1 - \mathbb{P}\left(-\epsilon \leq \frac{c_k^T \beta}{\sigma \sqrt{c_k^T (X^T V_y^{-1} X)^{-1} c_k}} \leq \epsilon \mid y, \sigma^2\right) \\ &= \Phi\left(-\epsilon + \frac{c_k^T \widehat{\beta}}{\sigma \sqrt{c_k^T (X^T V_y^{-1} X)^{-1} c_k}}\right) + \Phi\left(-\epsilon - \frac{c_k^T \widehat{\beta}}{\sigma \sqrt{c_k^T (X^T V_y^{-1} X)^{-1} c_k}}\right) \\ &= \Phi\left(\epsilon - \frac{\widehat{\sigma}}{\sigma} t_{\text{obs}}^{(k)}\right) + \Phi\left(\epsilon + \frac{\widehat{\sigma}}{\sigma} t_{\text{obs}}^{(k)}\right) \end{aligned}$$

where Φ denotes the standard normal CDF. We now use the following lemma.

Lemma 1. *Let $\epsilon > 0$, $c > 0$, $G : \mathbb{R} \rightarrow [0, 1]$ be a function such that $G'(x)$ is symmetric around zero and strictly decreasing in $|x|$, and let $h : \mathbb{R} \rightarrow [0, 1]$ be given by $h(x) = G(\epsilon - cx) + G(\epsilon + cx)$ for all $x \in \mathbb{R}$. Then, h is symmetric and if $x, y \in \mathbb{R}$, $h(x) > h(y)$ if and only if $|x| > |y|$.*

Proof. By assumption, $h'(x) = cG'(\epsilon + cx) - cG'(\epsilon - cx)$. Since $G'(x)$ is strictly decreasing in $|x|$, then if $x < 0$, $|\epsilon + cx| < |\epsilon - cx|$ and thus $h'(x) > 0$. If $x > 0$, then $|\epsilon + cx| > |\epsilon - cx|$, so $h'(x) < 0$. Furthermore, $h(-x) = G(\epsilon + cx) + G(\epsilon - cx) = h(x)$, so h is symmetric and strictly increases in $|x|$, which proves the claim.

By Lemma 1, since the standard normal PDF $\Phi'(x)$ is symmetric around zero and strictly decreasing in $|x|$ and $\widehat{\sigma}/\sigma > 0$, then

$$\mathbb{P}\left(\frac{|c_k^T \beta|}{\sigma \sqrt{c_k^T M c_k}} > \epsilon \mid y, \sigma^2\right) < \mathbb{P}\left(\frac{|c_{k'}^T \beta|}{\sigma \sqrt{c_{k'}^T M c_{k'}}} > \epsilon \mid y, \sigma^2\right) \iff |t_{\text{obs}}^{(k)}| < |t_{\text{obs}}^{(k')}|$$

for any $\epsilon > 0, \sigma^2 > 0$. If $|t_{\text{obs}}^{(k)}| < |t_{\text{obs}}^{(k')}|$, integrating out σ^2 preserves the order as

$$\begin{aligned} v_k(\epsilon) &= \mathbb{P}\left(\frac{|c_k^T \beta|}{\sigma \sqrt{c_k^T M c_k}} > \epsilon \mid y\right) = \int_0^\infty \mathbb{P}\left(\frac{|c_k^T \beta|}{\sigma \sqrt{c_k^T M c_k}} > \epsilon \mid y, \sigma^2\right) \pi(\sigma^2 \mid y) d\sigma^2 \\ &< \int_0^\infty \mathbb{P}\left(\frac{|c_{k'}^T \beta|}{\sigma \sqrt{c_{k'}^T M c_{k'}}} > \epsilon \mid y, \sigma^2\right) \pi(\sigma^2 \mid y) d\sigma^2 = \mathbb{P}\left(\frac{|c_{k'}^T \beta|}{\sigma \sqrt{c_{k'}^T M c_{k'}}} > \epsilon \mid y\right) = v_{k'}(\epsilon) \end{aligned}$$

which shows that $|t_{\text{obs}}^{(k)}| < |t_{\text{obs}}^{(k')}|$ implies $v_k(\epsilon) < v_{k'}(\epsilon)$ for all $\epsilon > 0$. If $v_k(\epsilon) < v_{k'}(\epsilon)$ for all $\epsilon > 0$, then this implies that there exists $\epsilon > 0, \sigma^2 > 0$ such that $\mathbb{P}\left(\frac{|c_k^T \beta|}{\sigma \sqrt{c_k^T M c_k}} > \epsilon \mid y, \sigma^2\right) < \mathbb{P}\left(\frac{|c_{k'}^T \beta|}{\sigma \sqrt{c_{k'}^T M c_{k'}}} > \epsilon \mid y, \sigma^2\right)$, which implies $|t_{\text{obs}}^{(k)}| < |t_{\text{obs}}^{(k')}|$ by the above argument. Therefore,

$$p_k > p_{k'} \iff |t_{\text{obs}}^{(k)}| < |t_{\text{obs}}^{(k')}| \iff \mathbb{P}\left(\frac{|c_k^T \beta|}{\sigma \sqrt{c_k^T M c_k}} > \epsilon \mid y, \sigma^2\right) < \mathbb{P}\left(\frac{|c_{k'}^T \beta|}{\sigma \sqrt{c_{k'}^T M c_{k'}}} > \epsilon \mid y, \sigma^2\right)$$

for all $\sigma^2 > 0$ and $\epsilon > 0$. The above inequality holds if and only if $v_k(\epsilon) < v_{k'}(\epsilon) \forall \epsilon > 0$.

S2. PROOF OF THEOREM 2.

The posterior conditional distributions for (2) are given by (3). Thus, we have $\gamma_\star \mid y, \rho, \sigma^2 \sim N_{n+p}(M_\star m_\star, \sigma^2 M_\star)$. For all $k = 1, \dots, K$, denote $\alpha_k = \frac{c_k^T M_\star m_\star}{\sqrt{c_k^T (X_\star^T V_{y_\star}^{-1} X_\star)^{-1} c_k}}$. Then,

$$\begin{aligned} \mathbb{P}\left(\frac{|c_k^T \gamma_\star|}{\sigma \sqrt{c_k^T (X_\star^T V_{y_\star}^{-1} X_\star)^{-1} c_k}} > \epsilon \mid y, \rho, \sigma^2\right) &= 1 - \mathbb{P}\left(-\epsilon \leq \frac{c_k^T \gamma_\star}{\sigma \sqrt{c_k^T (X_\star^T V_{y_\star}^{-1} X_\star)^{-1} c_k}} \leq \epsilon \mid y, \rho, \sigma^2\right) \\ &= \Phi\left(-\epsilon + \frac{\alpha_k}{\sigma}\right) + \Phi\left(-\epsilon - \frac{\alpha_k}{\sigma}\right). \end{aligned}$$

By Lemma 1, for any $k \neq k'$, $|\alpha_k| < |\alpha_{k'}|$ if and only if $\mathbb{P}\left(\frac{|c_k^T \gamma_\star|}{\sigma \sqrt{c_k^T (X_\star^T V_{y_\star}^{-1} X_\star)^{-1} c_k}} > \epsilon \mid y, \rho, \sigma^2\right) <$

$\mathbb{P}\left(\frac{|c_{k'}^T \gamma_\star|}{\sigma \sqrt{c_{k'}^T (X_\star^T V_{y_\star}^{-1} X_\star)^{-1} c_{k'}}} > \epsilon \mid y, \rho, \sigma^2\right)$ for all $\sigma^2 > 0, \epsilon > 0$. If there exists $\epsilon_\star > 0$ such that

$h_k(\epsilon_\star; \rho) < h_{k'}(\epsilon_\star; \rho)$, then there exists $\sigma^2 > 0$ such that $\mathbb{P}\left(\frac{|c_k^T \gamma_\star|}{\sigma \sqrt{c_k^T (X_\star^T V_{y_\star}^{-1} X_\star)^{-1} c_k}} > \epsilon_\star \mid y, \rho, \sigma^2\right) <$

$\mathbb{P} \left(\frac{|c_{k'}^T \gamma_\star|}{\sigma \sqrt{c_{k'}^T (X_\star^T V_{y_\star}^{-1} X_\star)^{-1} c_{k'}}} > \epsilon_\star \mid y, \rho, \sigma^2 \right)$, which implies $|\alpha_k| < |\alpha_{k'}|$. Thus, for any $\epsilon > 0$,

$$\begin{aligned} h_k(\epsilon; \rho) &= \int_0^\infty \mathbb{P} \left(\frac{|c_k^T \gamma_\star|}{\sigma \sqrt{c_k^T (X_\star^T V_{y_\star}^{-1} X_\star)^{-1} c_k}} > \epsilon \mid y, \rho, \sigma^2 \right) \pi(\sigma^2 \mid y, \rho) d\sigma^2 \\ &< \int_0^\infty \mathbb{P} \left(\frac{|c_{k'}^T \gamma_\star|}{\sigma \sqrt{c_{k'}^T (X_\star^T V_{y_\star}^{-1} X_\star)^{-1} c_{k'}}} > \epsilon \mid y, \rho, \sigma^2 \right) \pi(\sigma^2 \mid y, \rho) d\sigma^2 = h_{k'}(\epsilon; \rho), \end{aligned}$$

which completes the proof.

S3. METROPOLIS WITHIN GIBBS SAMPLING ALGORITHM FOR BYM2 MODEL

We present a Metropolis-Hastings within Gibbs sampling algorithm for obtaining posterior samples of $\{\beta, \gamma, \sigma^2, \rho\}$ from the model in (1) using the prior distribution

$$\pi(\beta, \gamma, \sigma^2, \rho) = N_n(\gamma \mid 0, \sigma^2 \rho V_\phi) \times \text{IG}(\sigma^2 \mid a_{\sigma^2}, b_{\sigma^2}) \times \text{PC}(\rho \mid \lambda_\rho, V_\phi).$$

In Algorithm S1, `chol` returns the upper triangular Cholesky factor of a positive definite matrix, `updateBeta` and `updateGamma` return β and γ from $\beta \mid y, \gamma, \sigma^2, \rho \sim N_p(F_\beta f_\beta, \sigma^2 F_\beta)$, where $F_\beta^{-1} = X^T X / (1 - \rho)$ and $f_\beta = X^T (y - \gamma) / (1 - \rho)$ and $\gamma \mid y, \beta, \sigma^2, \rho \sim N_n(F_\gamma f_\gamma, \sigma^2 F_\gamma)$, where $F_\gamma^{-1} = \frac{1}{1-\rho} I_n + \frac{1}{\rho} V_\phi^{-1}$ and $f_\gamma = (y - X\beta) / (1 - \rho)$, respectively, and `updateSigmaSq` samples $\sigma^2 \mid y, \beta, \gamma, \rho \sim \text{InvGamma} \left(a_{\sigma^2} + \frac{n}{2}, b_{\sigma^2} + \frac{\|y - X\beta - \gamma\|^2}{2(1-\rho)} \right)$.

Algorithm S1: Update steps for Metropolis-Hastings within Gibbs sampling of posterior of $(\beta, \gamma, \sigma^2, \rho)$ in BYM2 Model with flat β prior and PC ρ prior

Given $y, X, R = \text{chol}(X^T X), V_\phi^{-1}, m_1 = X^T y, P, \Lambda = \text{diag}(\lambda_1, \dots, \lambda_n), a_{\sigma^2}, b_{\sigma^2}, \lambda_\rho$:

function updateBeta(γ, σ^2, ρ):

for $i = 1, \dots, p$ **do**

 | Sample $z_i \sim N(0, \sigma^2(1 - \rho))$.

 Set $v_p \leftarrow \text{forwardsolve}(R^T, m_1 - X^T \gamma)$; $\beta \leftarrow \text{backsolve}(R, v_p + z)$.

return β .

function updateGamma(β, σ^2, ρ):

 Set $v_n \leftarrow y - X\beta$.

 Update $v_n \leftarrow \text{diag}\left(\frac{\rho}{\rho + (1 - \rho)\lambda_i}\right) P^T v_n$.

for $i = 1, \dots, n$ **do**

 | Sample $z_i \sim N(0, \sigma^2)$.

 Set $\gamma \leftarrow P\left(v_n + \text{diag}\left(\sqrt{\frac{\rho(1 - \rho)}{\rho + \lambda_i(1 - \rho)}}\right) z\right)$.

return γ .

function updateSigmaSq(ρ, r^2):

 Sample $\tau^2 \sim \Gamma\left(a_{\sigma^2} + \frac{n}{2}, b_{\sigma^2} + \frac{r^2}{2(1 - \rho)}\right)$; set $\sigma^2 \leftarrow 1/\tau^2$.

return σ^2 .

function MHupdateRho($\gamma, \sigma^2, \rho, r^2$):

 Initialize $\rho_\star \leftarrow 1$.

while $\rho_\star \geq 1$ **do**

 | Sample $\tau^2 \sim \Gamma\left(\frac{n}{2} - 1, \frac{r^2}{2\sigma^2}\right)$; set $\rho_\star \leftarrow 1 - 1/\tau^2$.

 Set $c_1 \leftarrow \sqrt{\sum_{i=1}^n \left(\frac{\rho}{\lambda_i} - \log\left(\frac{\rho}{\lambda_i} + (1 - \rho)\right)\right)} - n\rho$.

 Set $c_2 \leftarrow \sqrt{\sum_{i=1}^n \left(\frac{\rho_\star}{\lambda_i} - \log\left(\frac{\rho_\star}{\lambda_i} + (1 - \rho_\star)\right)\right)} - n\rho_\star$.

 Set $\alpha_{MH} \leftarrow \frac{n}{2} \log\left(\frac{\rho}{\rho_\star}\right) + \lambda_\rho (c_1 - c_2) + \frac{\gamma^T V_\phi^{-1} \gamma}{2\sigma^2} \left(\frac{1}{\rho} - \frac{1}{\rho_\star}\right)$.

 Sample $u \sim \text{Unif}(0, 1)$.

if $\log(u) \leq \alpha_{MH}$ **then return** ρ_\star .

else return ρ .

MHupdateRho updates ρ using a Metropolis-Hastings random walk by proposing $1 - \rho_\star \sim \text{TruncInvGamma}\left(\frac{n}{2} - 1, \frac{\|y - X\beta - \gamma\|^2}{2\sigma^2}, [0, 1]\right)$, where we denote $Z_1 \sim \text{TruncInvGamma}(a, b, [c_L, c_U])$, $a > 0, b > 0, 0 \leq c_L < c_U$ if $\mathbb{P}(Z_1 \leq z) = \mathbb{P}(Z_2 \leq z | c_L \leq Z_2 \leq c_U)$ with $Z_2 \sim \text{IG}(a, b)$. The Metropolis-Hastings acceptance probability is equal to $\min\{1, \exp(\alpha_{MH})\}$, where

$$\exp(\alpha_{MH}) = \frac{\pi(\beta, \gamma, \sigma^2, \rho_\star | y) Q(\rho_\star, \rho)}{\pi(\beta, \gamma, \sigma^2, \rho | y) Q(\rho, \rho_\star)},$$

4

α_{MH} is the acceptance log-ratio computed in Algorithm S1, and $Q(\rho, \rho_\star)$ is the proposal density for a new candidate ρ_\star . Expanding via Bayes' Rule yields

$$\exp(\alpha_{MH}) = \frac{\pi(\beta, \gamma, \sigma^2, \rho_\star | y) Q(\rho_\star, \rho)}{\pi(\beta, \gamma, \sigma^2, \rho | y) Q(\rho, \rho_\star)} = \frac{\pi(y | \beta, \gamma, \sigma^2, \rho_\star) \pi(\gamma | \sigma^2, \rho_\star) \pi(\rho_\star) Q(\rho_\star, \rho)}{\pi(y | \beta, \gamma, \sigma^2, \rho) \pi(\gamma | \sigma^2, \rho) \pi(\rho) Q(\rho, \rho_\star)}.$$

The Jacobian of the transformation $g(x) = 1 - x$ is constant and the proposal density $Q(\rho, \rho_\star) \propto (1 - \rho_\star)^{-n/2} \exp\left(-\frac{\|y - X\beta - \gamma\|^2}{2\sigma^2(1 - \rho_\star)}\right)$, hence $\frac{\pi(y | \beta, \gamma, \sigma^2, \rho_\star) Q(\rho_\star, \rho)}{\pi(y | \beta, \gamma, \sigma^2, \rho) Q(\rho, \rho_\star)} = 1$. The remaining terms in the ratio are the prior densities. The ratio $\frac{\pi(\gamma | \sigma^2, \rho_\star)}{\pi(\gamma | \sigma^2, \rho)} = \left(\frac{\rho_\star}{\rho}\right)^{-\frac{n}{2}} \exp\left(\frac{\gamma^T V_\phi^{-1} \gamma}{2\sigma^2} (1/\rho - 1/\rho_\star)\right)$ and $\pi(\rho_\star) = \text{PC}(\rho_\star | \lambda_\rho) \propto \lambda_\rho \exp(-\lambda_\rho d(\rho_\star; V_\phi))$. Here, $d(\rho_\star; V_\phi) = \sqrt{2D_{KL}(p(y; \rho_\star) || q(y))}$ and the Kullback-Leiber divergence of $p(y; \rho_\star) = N_n(y | 0_n, \rho_\star V_\phi + (1 - \rho_\star) I_n)$ from $q(y) = N_n(y | 0_n, I_n)$ is

$$D_{KL}(p(y; \rho_\star) || q(y)) = -\frac{n\rho_\star}{2} + \frac{\rho_\star}{2} \sum_{i=1}^n \frac{1}{\lambda_i} - \frac{1}{2} \sum_{i=1}^n \log(\rho_\star/\lambda_i + 1 - \rho_\star).$$

The acceptance ratio simplifies to

$$\exp(\alpha_{MH}) = \left(\frac{\rho_\star}{\rho}\right)^{-\frac{n}{2}} \exp\left(\frac{\gamma^T V_\phi^{-1} \gamma}{2\sigma^2} (1/\rho - 1/\rho_\star) + \lambda_\rho (d(\rho; V_\phi) - d(\rho_\star; V_\phi))\right).$$

Algorithm S2 invokes updating steps in Algorithm S1 to draw posterior samples of $\{\beta, \gamma, \sigma^2, \rho\}$ in a Gibbs sampling scheme with Metropolis random walk and obtains samples of $\phi = \frac{\gamma}{\sigma\sqrt{\rho}}$. For estimating difference boundaries, Algorithm S2 takes in $c_1, \dots, c_K \in \mathbb{R}^n$ corresponding to boundaries of interest. Simultaneous reduction at the start of Algorithm S2 increases computational efficiency and facilitates Monte Carlo estimation for ϵ -difference probabilities in (12). We compute $\Delta_k = \frac{c_k^T \phi}{\sqrt{c_k^T \text{Var}(\phi | y, \sigma^2, \rho) c_k}}$ for each posterior sample of $\{\phi, \rho\}$ and $k = 1, \dots, K$.

S4. CONSTRUCTION OF DIFFERENCE PROBABILITIES ON MODELED RESPONSE LEVEL

Suppose that the modeled response is $Y | \beta, \gamma, \sigma^2, \rho \sim N(X\beta + \gamma, \sigma^2(1 - \rho))$ and the prior is $\pi(\beta, \gamma, \sigma^2) = N(\gamma | 0, \sigma^2 \rho V_\phi) \times \text{IG}(\sigma^2 | a_{\sigma^2}, b_{\sigma^2})$. We begin by assuming that $0 \leq \rho \leq 1$ and positive definite V_ϕ are known. Denote $\gamma_\star = (\beta^T, \gamma^T)^T$.

Consider linear combinations of the modeled response $c_k^T Y$ where $c_1, \dots, c_K \in \mathbb{R}^n$. Let $\gamma_\star = (\beta, \gamma)^T$, and as discussed in Section 2.1, $\gamma_\star | \sigma^2, \rho \sim N(M_\star m_\star, \sigma^2 M_\star)$, $\sigma^2 | y, \rho \sim \text{IG}(a_n, b_n)$. Next,

$$Y | y, \sigma^2, \rho \sim N_n\left(\left(I_n - W V_1^{-1} W^T\right)^{-1} W V_1^{-1} W^T y, \sigma^2(1 - \rho) \left(I_n - W V_1^{-1} W^T\right)^{-1}\right),$$

Algorithm S2: Metropolis-Hastings within Gibbs sampling of posterior of $(\beta, \gamma, \sigma^2, \rho)$ in BYM2 Model with flat β prior and PC ρ prior

Given $y, X, R = \text{chol}(X^T X), I - H, V_\phi^{-1}, a_{\sigma^2}, b_{\sigma^2}, \lambda_\rho, \beta^{(0)}, \gamma^{(0)}, \sigma^{2(0)}, \rho^{(0)}, c_1, \dots, c_K$:

Set $U, D, P, \Lambda \leftarrow \text{simulReduce}(V_\phi^{-1}, I - H)$.

Precompute $m_1 \leftarrow X^T y$.

for $k = 1, \dots, K$ **do**

 | Set $\omega_k \leftarrow U^T c_k$.

for $t = 1, \dots, T$ **do**

 | Set $\beta^{(t)} \leftarrow \text{updateBeta}(\gamma^{(t-1)}, \sigma^{2(t-1)}, \rho^{(t-1)})$.

 | Set $\gamma^{(t)} \leftarrow \text{updateGamma}(\beta^{(t)}, \sigma^{2(t-1)}, \rho^{(t-1)})$.

 | Set $r^{2(t)} \leftarrow \|y - X\beta^{(t)} - \gamma^{(t)}\|^2$.

 | Set $\sigma^{2(t)} \leftarrow \text{updateSigmaSq}(\rho^{(t-1)}, r^{2(t)})$.

 | Set $\rho^{(t)} \leftarrow \text{MHupdateRho}(\gamma^{(t)}, \sigma^{2(t)}, \rho^{(t-1)}, r^{2(t)})$.

 | Set $\phi^{(t)} \leftarrow \gamma^{(t)} / (\sigma^{(t)} \sqrt{\rho^{(t)}})$.

for $k = 1, \dots, K$ **do**

 | Set $\Delta_k^{(t)} = \left(\omega_k^T \text{diag} \left(\frac{1 - \rho^{(t)}}{1 + \rho^{(t)}(d_i - 1)} \right) \omega_k \right)^{-1/2} c_k^T \phi^{(t)}$.

function $\text{simulReduce}(A, B)$:

 | Solve spectral decomposition $A = P\Lambda P^T$ and set $A^{-1/2} \leftarrow P\Lambda^{-1/2}P^T$.

 | Solve spectral decomposition $A^{-1/2}BA^{-1/2} = CDC^T$ and set $U \leftarrow A^{-1/2}C$.

return U, D, P, Λ .

where $WV_1^{-1}W^T = \frac{1}{2}H + (I_n - H)(B + I_n - H)^{-1}(I_n - H)$, $B = I_n - H + \frac{1-\rho}{\rho}V_\phi^{-1}$ and V_ϕ is assumed to be positive definite. For $\epsilon > 0$, define the conditional ϵ -difference probabilities as

$$h_k(\epsilon; \rho) = \mathbb{P} \left(\frac{|c_k^T Y| / \sqrt{\sigma^2(1 - \rho)}}{\sqrt{c_k^T (I_n - WV_1^{-1}W^T)^{-1} c_k}} > \epsilon \mid y, \rho \right)$$

for $k = 1, \dots, K$. Let $0 \neq c_i, c_j \in \mathbb{R}^n$ and set $\alpha_i = \frac{\mathbb{E}(c_i^T Y \mid y, \sigma^2, \rho)}{\sqrt{\text{Var}(c_i^T Y \mid y, \sigma^2, \rho)}} = \frac{c_i^T (I_n - WV_1^{-1}W^T)^{-1} WV_1^{-1} y}{\sqrt{(1 - \rho) c_i^T (I_n - WV_1^{-1}W^T)^{-1} c_i}}$. We

show that the rankings of these posterior probabilities are stable by proving that given two vectors $c_i, c_j \in \mathbb{R}^n, 0 < \rho < 1$, if the corresponding conditional probabilities satisfy $h_i(\epsilon; \rho) < h_j(\epsilon; \rho)$

for some $\epsilon > 0$, then $h_i(\epsilon; \rho) < h_j(\epsilon; \rho)$ for all $\epsilon > 0$. First, define

$$\begin{aligned} w_i(\epsilon; \sigma^2, \rho) &= \mathbb{P} \left(\frac{|c_i^T Y| / \sqrt{\sigma^2(1-\rho)}}{\sqrt{c_i^T (I_n - W V_1^{-1} W^T)^{-1} c_i}} > \epsilon \mid y, \sigma^2, \rho \right) \\ &= \mathbb{P} \left(-\epsilon - \frac{\alpha_i}{\sigma} \leq Z \leq \epsilon - \frac{\alpha_i}{\sigma} \right), \quad Z \sim N(0, 1) \\ &= \Phi \left(-\epsilon + \frac{\alpha_i}{\sigma} \right) + \Phi \left(-\epsilon - \frac{\alpha_i}{\sigma} \right) \end{aligned}$$

where Φ denotes the standard normal CDF. Let $f : \mathbb{R} \rightarrow \mathbb{R}$ be given by $f(x) = \Phi(-\epsilon + \frac{x}{\sigma}) + \Phi(-\epsilon - \frac{x}{\sigma})$ for any $\sigma > 0$. Then, as shown in Appendix S1, for any $x, y \in \mathbb{R}$, $|x| > |y|$ if and only if $f(x) > f(y)$. Therefore, for any $\sigma^2 > 0$, $w_i(\epsilon; \sigma^2, \rho) > w_j(\epsilon; \sigma^2, \rho)$ if and only if $|\alpha_i(\sigma^2)| > |\alpha_j(\sigma^2)|$. Thus, if $|\alpha_i| > |\alpha_j|$, then

$$h_i(\epsilon; \rho) = \int_0^\infty w_i(\epsilon; \sigma^2, \rho) \pi(\sigma^2 \mid y) d\sigma^2 < \int_0^\infty w_j(\epsilon; \sigma^2, \rho) \pi(\sigma^2 \mid y) d\sigma^2 = h_j(\epsilon; \rho)$$

for all $\epsilon > 0$. Likewise, if $h_i(\epsilon; \rho) < h_j(\epsilon; \rho)$ for all ϵ , then there exists $\epsilon > 0, \sigma^2 > 0$ such that $w_i(\epsilon; \sigma^2, \rho) > w_j(\epsilon; \sigma^2, \rho)$, which implies $|\alpha_i| > |\alpha_j|$. Since the statement $|\alpha_i| > |\alpha_j|$ does not depend on ϵ , we conclude that if $h_i(\epsilon; \rho) < h_j(\epsilon; \rho)$ for some given $\epsilon > 0$, then $h_i(\epsilon; \rho) < h_j(\epsilon; \rho)$ for all $\epsilon > 0$.

Similar to the ϵ -difference probabilities on the effects level, one can define the corresponding marginal posterior ϵ -difference probabilities as

$$v_k(\epsilon) = \mathbb{P} \left(\frac{|c_k^T Y| / \sqrt{\sigma^2(1-\rho)}}{\sqrt{c_k^T (I_n - W V_1^{-1} W^T)^{-1} c_k}} > \epsilon \mid y \right).$$

S5. SENSITIVITY ANALYSIS OF DIFFERENCE THRESHOLD

We assess the effect of different values of the difference threshold ϵ in our proposed framework for detecting spatial disparities in a simulation experiment with a generated map using 3,078 contiguous U.S. counties. We use (1) and construct $V_\phi^{-1} = c(D_W - \alpha W)$ with W encoding the neighbors of U.S. counties. We generate the spatial random effects ϕ using $\alpha = 0.99$, scaling factor $c = 0.365$, and covariates $X = (1_n, x)$, where $x \sim N_n(0, I_n)$ and simulate the observed data y using (1) with $\sigma^2 = 4$, $\rho = 0.93$, and $\beta = (2, 5)^T$. For the simulated data, there are $K = 9,119$ distinct pairs of adjacent counties. We investigate spatial difference boundary detection on the set of all pairs of neighboring counties, $L = \{(i, j) : i < j, i \sim j\}$. The indicator of a true difference boundary for a neighboring pair (i, j) and a given difference threshold ϵ is defined as

$$r_{ij}(\epsilon) = \mathbb{I} \left(\frac{|\phi_i - \phi_j|}{\sqrt{c_{ij}^T \text{Var}(\phi \mid y, \sigma^2, \rho) c_{ij}}} > \epsilon \right), \text{ evaluated using the true values of } \phi \text{ and } \rho.$$

We analyze the simulated data using the BYM2 model in (1) and the prior $\pi(\beta, \gamma, \sigma^2, \rho) = N_n(\gamma | 0, \sigma^2 \rho V_\phi) \times \text{IG}(\sigma^2 | 0.1, 0.1) \times \text{PC}(\rho | .0335, V_\phi)$, where $\lambda_\rho = 0.0335$ is chosen such that $\mathbb{P}(\rho \leq 0.5) \approx \frac{2}{3}$. We use Algorithm S2 to obtain 30,000 samples from the joint posterior of $\{\beta, \gamma, \sigma^2, \rho\}$ after discarding 10,000 burn-in samples. We then compute Monte Carlo estimates of $\{v_{ij}(\epsilon)\}_{(i,j) \in L}$ using (12) and minimize the conditional entropy loss function in (18) to obtain $\epsilon_{CE} = 1.685$ as the optimal difference threshold. For this difference threshold, there are 4,841 true difference boundaries, that is $\sum_{(i,j), i \sim j} r_{ij}(\epsilon_{CE}) = 4,841$. We compute $t^* = 0.855$ using (17) with a Bayesian FDR tolerance of $\delta = 0.05$ and report 2839 county boundaries as spatial disparities.

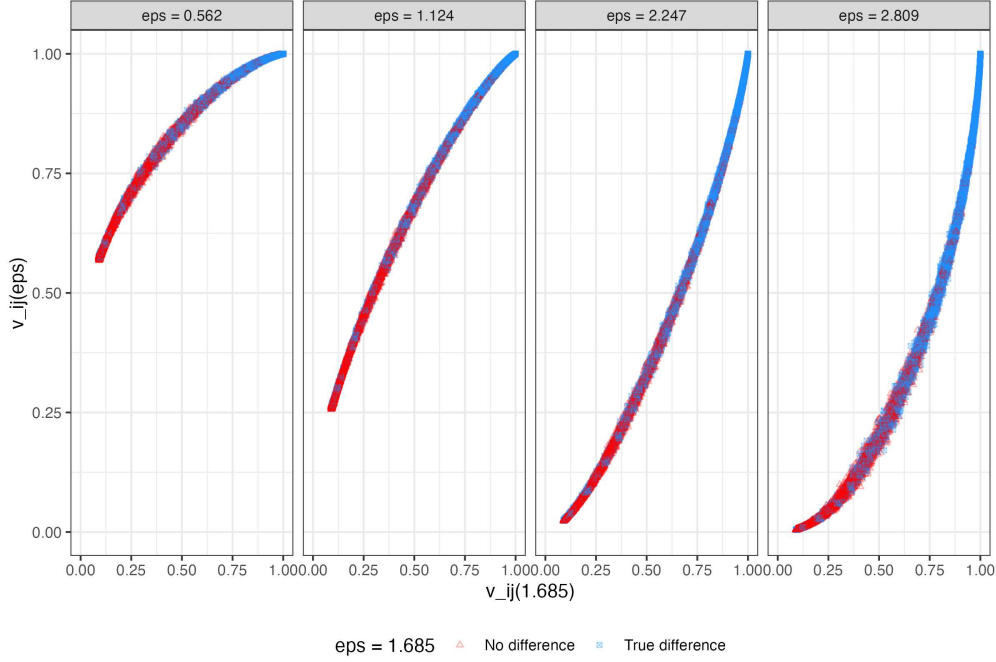


FIGURE S1. Difference probabilities $\{v_{ij}(\epsilon)\}_{(i,j) \in L}$ computed using simulated US county map and difference thresholds $\epsilon = 0.562, 1.124, 2.247, 2.809$ versus $\{v_{ij}(1.685)\}_{(i,j) \in L}$. Difference probabilities corresponding to true difference boundaries for a $\epsilon_{CE} = 1.685$ threshold are colored in blue while non-difference boundaries are colored in red.

To analyze the effect of the value of ϵ on difference boundary detection, we repeat the above process for $\epsilon = 0.562, 1.124, 2.247, 2.809$. Figure S1 shows each set of difference probabilities $\{v_{ij}(\epsilon)\}_{(i,j), i \sim j}$ plotted on the y-axis against $\{v_{ij}(\epsilon_{CE})\}_{(i,j), i \sim j}$ on the x-axis. Decreasing the difference threshold relative to ϵ_{CE} generally increases each difference probability as shown in the left two panels, while increasing the difference threshold decreases each difference probability, as seen in the right two graphs. Table S1 shows the resulting number of detected boundaries, the number of true boundaries or $\sum_{(i,j), i \sim j} r_{ij}(\epsilon)$, the sensitivity or true positive rate, the specificity or true negative rate, and the overall accuracy for each difference threshold ϵ . As the difference

| ϵ | t^\star | Detected Boundaries | True Boundaries | Sensitivity | Specificity | Accuracy |
|--------------|-----------|---------------------|-----------------|-------------|-------------|----------|
| 0.562 | 0.811 | 6070 | 7609 | 0.742 | 0.721 | 0.739 |
| 1.124 | 0.832 | 4212 | 6188 | 0.638 | 0.909 | 0.725 |
| 1.685 | 0.856 | 2838 | 4841 | 0.553 | 0.962 | 0.745 |
| 2.247 | 0.874 | 1756 | 3679 | 0.454 | 0.985 | 0.771 |
| 2.809 | 0.886 | 983 | 2674 | 0.352 | 0.994 | 0.806 |

TABLE S1. Cutoff probabilities, number of detected/true difference boundaries, and classification performance with Bayesian FDR tolerance $\delta = 0.05$ across different values of difference threshold ϵ . The difference threshold $\epsilon_{CE} = 1.685$ (bolded) is found from minimizing the conditional entropy loss function in (18).

threshold ϵ increases, the number of detected and true difference boundaries both decrease and the sensitivity decreases while the specificity increases. The entropy based choice provides a middle ground between classifying all or no boundaries as disparities.

S6. IMPACT OF UNCERTAINTY IN SPATIAL VARIANCE PROPORTION

We investigate the effect of uncertainty in ρ , the spatial proportion of variance, by reanalyzing the simulated dataset in Section S5 using a fixed value of ρ . We fix $\rho = 0.93$ and draw 10,000 exact samples from $\pi(\beta, \gamma, \sigma^2 | y, \rho)$ using (3). For each boundary between counties, we compute a Monte Carlo estimate of the difference probability $h_{ij}(\epsilon; \rho)$ as defined in 10. Minimizing the conditional entropy loss in (18) yields the optimal difference threshold of $\epsilon = 1.296$, which corresponds to 5750 true difference boundaries. For a Bayesian FDR tolerance of $\delta = 0.05$, the optimal probability cut-off point is $t^\star = 0.8092$, which results in reporting 3,524 pairs of neighboring counties as spatial disparities with a sensitivity of 0.583 and specificity of 0.949.

The left panel of Figure S2 shows the ROC curves for the model discussed in Section S5 with a PC prior on ρ and difference threshold $\epsilon = 1.685$ in orange and the conditioned model with difference threshold $\epsilon = 1.296$. Although the model conditioned on the true value of ρ results in reporting a greater number of difference boundaries, the model that incorporates uncertainty in the spatial proportion of variance results in slightly superior classification performance (AUC = 0.883) than the conditioned model (AUC = 0.862). The right panel of Figure S2 shows a scatterplot of the difference probabilities in each model. The two sets of difference probabilities are highly correlated ($r = 0.995$) and difference probabilities corresponding to true difference boundaries are generally larger in the conditioned model. Therefore, uncertainty in ρ does not appear to negatively impact classification performance but does result in more conservative classification under equivalent control of the Bayesian FDR.

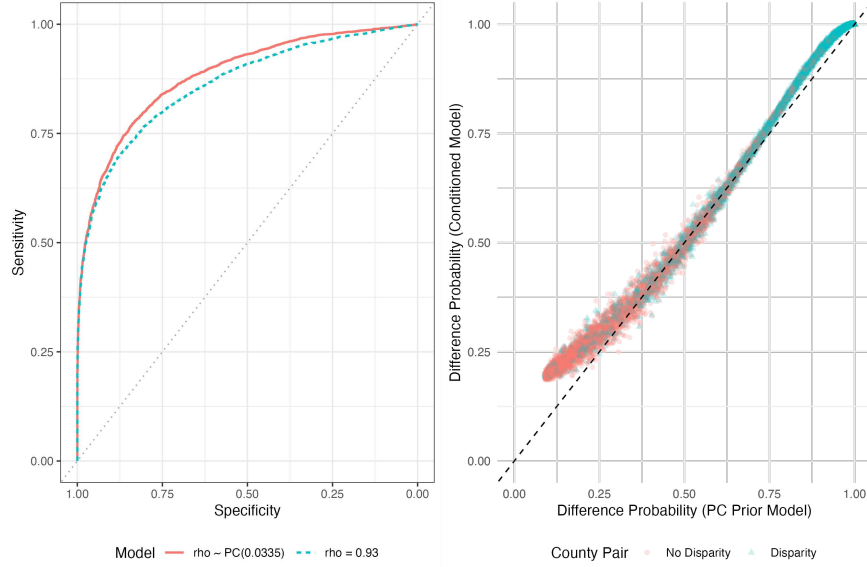


FIGURE S2. Left: ROC curves for simulated data analysis with a BYM2 model conditioned on $\rho = 0.93$ and difference threshold $\epsilon = 1.296$ versus analysis with a BYM2 model with a PC prior on ρ and $\epsilon = 1.685$. Right: Difference probabilities conditioned on $\rho = 0.93$ versus difference probabilities from analysis with a PC prior on ρ . Points above the dotted line indicate neighboring pairs with difference probabilities that are greater in the conditioned model than the PC prior model.

S7. CLASSIFIED SPATIAL DISPARITIES IN COUNTY-LEVEL TRACHEAL, BRONCHUS, AND LUNG CANCER MORTALITY RATES

In Section 5, we apply the maximum conditional entropy criterion to select the difference threshold $\epsilon_{CE} = 0.922$ and set the Bayesian FDR tolerance at $\delta = 0.05$ to obtain 722 out of 8,793 pairs of geographically adjacent counties within the continental US as local spatial disparities. The complete list of disparities is shown in Table S2, along with the Monte Carlo estimates of

$$v_k(\epsilon_{CE}) = \mathbb{P} \left(\frac{|a_k^T \phi|}{\sqrt{a_k^T \text{Var}(\phi | y, \rho) a_k}} > \epsilon \mid y \right).$$

| | County 1 | County 2 | $v_k(\epsilon_{CE})$ |
|---|--------------------------|---------------------------|----------------------|
| 1 | Alachua County, Florida | Union County, Florida | 1.000 |
| 2 | Baker County, Florida | Union County, Florida | 1.000 |
| 3 | Bradford County, Florida | Union County, Florida | 1.000 |
| 4 | Columbia County, Florida | Union County, Florida | 1.000 |
| 5 | Boone County, Kentucky | Gallatin County, Kentucky | 1.000 |
| 6 | Carroll County, Kentucky | Gallatin County, Kentucky | 1.000 |
| 7 | Clark County, Kentucky | Powell County, Kentucky | 1.000 |

| | | | |
|----|--------------------------------|---------------------------------|-------|
| 8 | Menifee County, Kentucky | Powell County, Kentucky | 1.000 |
| 9 | Montgomery County, Kentucky | Powell County, Kentucky | 1.000 |
| 10 | Attala County, Mississippi | Madison County, Mississippi | 1.000 |
| 11 | Hinds County, Mississippi | Madison County, Mississippi | 1.000 |
| 12 | Holmes County, Mississippi | Madison County, Mississippi | 1.000 |
| 13 | Leake County, Mississippi | Madison County, Mississippi | 1.000 |
| 14 | Madison County, Mississippi | Rankin County, Mississippi | 1.000 |
| 15 | Madison County, Mississippi | Scott County, Mississippi | 1.000 |
| 16 | Madison County, Mississippi | Yazoo County, Mississippi | 1.000 |
| 17 | Pierce County, North Dakota | Rolette County, North Dakota | 1.000 |
| 18 | Muskingum County, Ohio | Noble County, Ohio | 1.000 |
| 19 | Jeff Davis County, Georgia | Wheeler County, Georgia | 1.000 |
| 20 | Switzerland County, Indiana | Gallatin County, Kentucky | 1.000 |
| 21 | Pike County, Kentucky | Buchanan County, Virginia | 1.000 |
| 22 | Caldwell Parish, Louisiana | Franklin Parish, Louisiana | 1.000 |
| 23 | Lee County, Mississippi | Union County, Mississippi | 1.000 |
| 24 | Anson County, North Carolina | Marlboro County, South Carolina | 1.000 |
| 25 | Noble County, Ohio | Washington County, Ohio | 1.000 |
| 26 | Gallatin County, Kentucky | Owen County, Kentucky | 1.000 |
| 27 | McCreary County, Kentucky | Wayne County, Kentucky | 1.000 |
| 28 | Martin County, Kentucky | Wayne County, West Virginia | 1.000 |
| 29 | Frederick County, Virginia | Hardy County, West Virginia | 1.000 |
| 30 | Bottineau County, North Dakota | Rolette County, North Dakota | 1.000 |
| 31 | Guernsey County, Ohio | Noble County, Ohio | 1.000 |
| 32 | Chattahoochee County, Georgia | Marion County, Georgia | 1.000 |
| 33 | Jackson County, Kentucky | Owsley County, Kentucky | 1.000 |
| 34 | Cumberland County, Tennessee | Fentress County, Tennessee | 1.000 |
| 35 | Boone County, West Virginia | Raleigh County, West Virginia | 1.000 |
| 36 | Bell County, Kentucky | Leslie County, Kentucky | 1.000 |
| 37 | Rolette County, North Dakota | Towner County, North Dakota | 1.000 |
| 38 | Laurel County, Kentucky | McCreary County, Kentucky | 1.000 |
| 39 | Gallatin County, Kentucky | Grant County, Kentucky | 0.999 |
| 40 | Caldwell Parish, Louisiana | Ouachita Parish, Louisiana | 0.999 |
| 41 | Allen Parish, Louisiana | Vernon Parish, Louisiana | 0.999 |
| 42 | Robeson County, North Carolina | Marlboro County, South Carolina | 0.999 |
| 43 | Clay County, Kentucky | Perry County, Kentucky | 0.999 |
| 44 | Johnson County, Kentucky | Morgan County, Kentucky | 0.999 |
| 45 | Madison County, Missouri | Perry County, Missouri | 0.999 |

| | | | |
|----|-------------------------------------|----------------------------------|-------|
| 46 | Choctaw County, Mississippi | Webster County, Mississippi | 0.999 |
| 47 | Morgan County, Kentucky | Wolfe County, Kentucky | 0.999 |
| 48 | Lee County, Mississippi | Pontotoc County, Mississippi | 0.999 |
| 49 | Haakon County, South Dakota | Ziebach County, South Dakota | 0.999 |
| 50 | Wayne County, Kentucky | Scott County, Tennessee | 0.999 |
| 51 | Boyd County, Kentucky | Lawrence County, Kentucky | 0.999 |
| 52 | Anderson County, Tennessee | Scott County, Tennessee | 0.999 |
| 53 | Florence County, South Carolina | Marlboro County, South Carolina | 0.999 |
| 54 | McCreary County, Kentucky | Pulaski County, Kentucky | 0.999 |
| 55 | Pendleton County, West Virginia | Pocahontas County, West Virginia | 0.999 |
| 56 | Lampasas County, Texas | San Saba County, Texas | 0.998 |
| 57 | Anderson County, Texas | Cherokee County, Texas | 0.998 |
| 58 | Fulton County, Kentucky | Hickman County, Kentucky | 0.998 |
| 59 | Carter County, Missouri | Oregon County, Missouri | 0.998 |
| 60 | Clay County, Kentucky | Owsley County, Kentucky | 0.998 |
| 61 | Pickett County, Tennessee | Scott County, Tennessee | 0.998 |
| 62 | Grand County, Utah | San Juan County, Utah | 0.998 |
| 63 | Hardin County, Illinois | Pope County, Illinois | 0.998 |
| 64 | Knott County, Kentucky | Perry County, Kentucky | 0.997 |
| 65 | Morgan County, Ohio | Noble County, Ohio | 0.997 |
| 66 | Sheridan County, Montana | Divide County, North Dakota | 0.997 |
| 67 | Lee County, Mississippi | Prentiss County, Mississippi | 0.997 |
| 68 | Lincoln County, Tennessee | Moore County, Tennessee | 0.997 |
| 69 | Buchanan County, Virginia | Mingo County, West Virginia | 0.997 |
| 70 | Anderson County, Texas | Houston County, Texas | 0.997 |
| 71 | Effingham County, Georgia | Jasper County, South Carolina | 0.997 |
| 72 | Jeff Davis County, Georgia | Telfair County, Georgia | 0.997 |
| 73 | Meriwether County, Georgia | Pike County, Georgia | 0.997 |
| 74 | Craighead County, Arkansas | Poinsett County, Arkansas | 0.997 |
| 75 | Bryan County, Georgia | Chatham County, Georgia | 0.997 |
| 76 | Crowley County, Colorado | Kiowa County, Colorado | 0.997 |
| 77 | Sumner County, Tennessee | Trousdale County, Tennessee | 0.997 |
| 78 | Shenandoah County, Virginia | Hardy County, West Virginia | 0.997 |
| 79 | Chesterfield County, South Carolina | Marlboro County, South Carolina | 0.997 |
| 80 | Lee County, Mississippi | Monroe County, Mississippi | 0.997 |
| 81 | Dooly County, Georgia | Houston County, Georgia | 0.997 |
| 82 | Bienville Parish, Louisiana | Red River Parish, Louisiana | 0.996 |
| 83 | Monroe County, Ohio | Noble County, Ohio | 0.996 |

| | | | |
|-----|----------------------------------|---------------------------------|-------|
| 84 | Coffee County, Tennessee | Moore County, Tennessee | 0.996 |
| 85 | Hickman County, Tennessee | Williamson County, Tennessee | 0.996 |
| 86 | Magoffin County, Kentucky | Morgan County, Kentucky | 0.996 |
| 87 | Boone County, West Virginia | Kanawha County, West Virginia | 0.996 |
| 88 | Apache County, Arizona | Montezuma County, Colorado | 0.996 |
| 89 | Richmond County, North Carolina | Marlboro County, South Carolina | 0.996 |
| 90 | Jefferson County, Indiana | Scott County, Indiana | 0.996 |
| 91 | Belmont County, Ohio | Noble County, Ohio | 0.996 |
| 92 | Chattahoochee County, Georgia | Webster County, Georgia | 0.996 |
| 93 | Letcher County, Kentucky | Dickenson County, Virginia | 0.995 |
| 94 | East Feliciana Parish, Louisiana | Amite County, Mississippi | 0.995 |
| 95 | Estill County, Kentucky | Powell County, Kentucky | 0.995 |
| 96 | Jefferson County, Alabama | Walker County, Alabama | 0.995 |
| 97 | Caldwell Parish, Louisiana | Richland Parish, Louisiana | 0.995 |
| 98 | Dade County, Georgia | Hamilton County, Tennessee | 0.995 |
| 99 | Arkansas County, Arkansas | Lincoln County, Arkansas | 0.995 |
| 100 | Breathitt County, Kentucky | Knott County, Kentucky | 0.994 |
| 101 | Craighead County, Arkansas | Dunklin County, Missouri | 0.994 |
| 102 | Dewey County, Oklahoma | Major County, Oklahoma | 0.994 |
| 103 | Carter County, Missouri | Reynolds County, Missouri | 0.994 |
| 104 | Montgomery County, Georgia | Wheeler County, Georgia | 0.994 |
| 105 | Burnet County, Texas | Lampasas County, Texas | 0.994 |
| 106 | Breathitt County, Kentucky | Magoffin County, Kentucky | 0.994 |
| 107 | Bradley County, Tennessee | Polk County, Tennessee | 0.994 |
| 108 | Issaquena County, Mississippi | Sharkey County, Mississippi | 0.994 |
| 109 | Greene County, Arkansas | Dunklin County, Missouri | 0.993 |
| 110 | Clark County, Indiana | Scott County, Indiana | 0.993 |
| 111 | Bacon County, Georgia | Coffee County, Georgia | 0.993 |
| 112 | Cleburne County, Alabama | Randolph County, Alabama | 0.993 |
| 113 | Meade County, South Dakota | Ziebach County, South Dakota | 0.993 |
| 114 | Coshocton County, Ohio | Holmes County, Ohio | 0.993 |
| 115 | Chase County, Kansas | Marion County, Kansas | 0.993 |
| 116 | Lampasas County, Texas | Mills County, Texas | 0.993 |
| 117 | Gilmer County, Georgia | Murray County, Georgia | 0.993 |
| 118 | Jackson County, Kentucky | Lee County, Kentucky | 0.992 |
| 119 | Apache County, Arizona | Greenlee County, Arizona | 0.992 |
| 120 | Benson County, North Dakota | Nelson County, North Dakota | 0.992 |
| 121 | Eddy County, New Mexico | Loving County, Texas | 0.992 |

| | | | |
|-----|-----------------------------------|----------------------------------|-------|
| 122 | Morgan County, Tennessee | Scott County, Tennessee | 0.992 |
| 123 | Mesa County, Colorado | San Juan County, Utah | 0.992 |
| 124 | Cherokee County, North Carolina | Polk County, Tennessee | 0.991 |
| 125 | Anderson County, Texas | Freestone County, Texas | 0.991 |
| 126 | Franklin County, Illinois | Perry County, Illinois | 0.991 |
| 127 | Benton County, Missouri | Camden County, Missouri | 0.991 |
| 128 | Bullitt County, Kentucky | Hardin County, Kentucky | 0.991 |
| 129 | McKinley County, New Mexico | Sandoval County, New Mexico | 0.991 |
| 130 | Jefferson County, Texas | Liberty County, Texas | 0.991 |
| 131 | Posey County, Indiana | Union County, Kentucky | 0.991 |
| 132 | Scott County, Indiana | Washington County, Indiana | 0.991 |
| 133 | Frederick County, Virginia | Hampshire County, West Virginia | 0.991 |
| 134 | Bienville Parish, Louisiana | Claiborne Parish, Louisiana | 0.991 |
| 135 | Reynolds County, Missouri | Wayne County, Missouri | 0.991 |
| 136 | Dyer County, Tennessee | Lake County, Tennessee | 0.990 |
| 137 | Clinton County, Missouri | DeKalb County, Missouri | 0.990 |
| 138 | Worcester County, Maryland | Accomack County, Virginia | 0.990 |
| 139 | Chickasaw County, Mississippi | Lee County, Mississippi | 0.990 |
| 140 | Letcher County, Kentucky | Perry County, Kentucky | 0.989 |
| 141 | Brown County, Illinois | Cass County, Illinois | 0.989 |
| 142 | Lawrence County, Kentucky | Wayne County, West Virginia | 0.989 |
| 143 | Crawford County, Iowa | Harrison County, Iowa | 0.989 |
| 144 | Gallatin County, Illinois | Posey County, Indiana | 0.988 |
| 145 | Burt County, Nebraska | Cuming County, Nebraska | 0.988 |
| 146 | Clearwater County, Idaho | Shoshone County, Idaho | 0.988 |
| 147 | Jackson County, Indiana | Scott County, Indiana | 0.988 |
| 148 | Dewey County, South Dakota | Ziebach County, South Dakota | 0.988 |
| 149 | Holmes County, Ohio | Knox County, Ohio | 0.988 |
| 150 | Barry County, Missouri | McDonald County, Missouri | 0.988 |
| 151 | Darlington County, South Carolina | Marlboro County, South Carolina | 0.988 |
| 152 | Bleckley County, Georgia | Pulaski County, Georgia | 0.988 |
| 153 | Coffee County, Georgia | Jeff Davis County, Georgia | 0.987 |
| 154 | Camden County, Missouri | Pulaski County, Missouri | 0.987 |
| 155 | Richmond County, Georgia | Edgefield County, South Carolina | 0.987 |
| 156 | Highland County, Virginia | Pendleton County, West Virginia | 0.987 |
| 157 | Carroll County, Mississippi | Grenada County, Mississippi | 0.987 |
| 158 | Angelina County, Texas | Polk County, Texas | 0.987 |
| 159 | Harlan County, Kentucky | Wise County, Virginia | 0.987 |

| | | | |
|-----|----------------------------------|---------------------------------|-------|
| 160 | Peach County, Georgia | Taylor County, Georgia | 0.987 |
| 161 | Tallahatchie County, Mississippi | Yalobusha County, Mississippi | 0.987 |
| 162 | Bent County, Colorado | Prowers County, Colorado | 0.987 |
| 163 | Trousdale County, Tennessee | Wilson County, Tennessee | 0.987 |
| 164 | Glades County, Florida | Okeechobee County, Florida | 0.986 |
| 165 | Clay County, Kentucky | Leslie County, Kentucky | 0.986 |
| 166 | Bedford County, Tennessee | Moore County, Tennessee | 0.986 |
| 167 | Grainger County, Tennessee | Jefferson County, Tennessee | 0.986 |
| 168 | Union County, New Mexico | Cimarron County, Oklahoma | 0.986 |
| 169 | Monroe County, Arkansas | Saint Francis County, Arkansas | 0.986 |
| 170 | Pasco County, Florida | Sumter County, Florida | 0.986 |
| 171 | Hickman County, Kentucky | Mississippi County, Missouri | 0.986 |
| 172 | Harrison County, Iowa | Shelby County, Iowa | 0.986 |
| 173 | Marion County, Florida | Sumter County, Florida | 0.986 |
| 174 | Issaquena County, Mississippi | Washington County, Mississippi | 0.986 |
| 175 | Cheatham County, Tennessee | Williamson County, Tennessee | 0.985 |
| 176 | Lake County, Tennessee | Obion County, Tennessee | 0.985 |
| 177 | Blount County, Alabama | Walker County, Alabama | 0.985 |
| 178 | Comanche County, Kansas | Woods County, Oklahoma | 0.985 |
| 179 | Macon County, Georgia | Peach County, Georgia | 0.985 |
| 180 | Pulaski County, Missouri | Texas County, Missouri | 0.985 |
| 181 | La Paz County, Arizona | Mohave County, Arizona | 0.985 |
| 182 | Tuscaloosa County, Alabama | Walker County, Alabama | 0.984 |
| 183 | Randolph County, West Virginia | Webster County, West Virginia | 0.984 |
| 184 | Perry County, Missouri | Saint Francois County, Missouri | 0.984 |
| 185 | Laurel County, Kentucky | Whitley County, Kentucky | 0.984 |
| 186 | Leake County, Mississippi | Neshoba County, Mississippi | 0.984 |
| 187 | Union County, Arkansas | Claiborne Parish, Louisiana | 0.984 |
| 188 | Dooly County, Georgia | Macon County, Georgia | 0.984 |
| 189 | Desha County, Arkansas | Coahoma County, Mississippi | 0.983 |
| 190 | Walker County, Georgia | Hamilton County, Tennessee | 0.983 |
| 191 | Breathitt County, Kentucky | Wolfe County, Kentucky | 0.983 |
| 192 | Macon County, Tennessee | Sumner County, Tennessee | 0.983 |
| 193 | Marion County, Kentucky | Washington County, Kentucky | 0.983 |
| 194 | Clark County, Kentucky | Estill County, Kentucky | 0.982 |
| 195 | Live Oak County, Texas | San Patricio County, Texas | 0.982 |
| 196 | Bell County, Kentucky | Harlan County, Kentucky | 0.982 |
| 197 | Union County, New Mexico | Dallam County, Texas | 0.982 |

| | | | |
|-----|---------------------------------|----------------------------------|-------|
| 198 | Ben Hill County, Georgia | Wilcox County, Georgia | 0.982 |
| 199 | Murray County, Georgia | Bradley County, Tennessee | 0.981 |
| 200 | Grenada County, Mississippi | Montgomery County, Mississippi | 0.981 |
| 201 | Bee County, Texas | Refugio County, Texas | 0.981 |
| 202 | Baker County, Georgia | Decatur County, Georgia | 0.981 |
| 203 | Citrus County, Florida | Sumter County, Florida | 0.981 |
| 204 | Leake County, Mississippi | Winston County, Mississippi | 0.981 |
| 205 | East Carroll Parish, Louisiana | Issaquena County, Mississippi | 0.980 |
| 206 | Lee County, Arkansas | Monroe County, Arkansas | 0.980 |
| 207 | Gilmer County, Georgia | Gordon County, Georgia | 0.980 |
| 208 | Franklin County, Kentucky | Shelby County, Kentucky | 0.980 |
| 209 | Allen Parish, Louisiana | Beauregard Parish, Louisiana | 0.980 |
| 210 | Caldwell Parish, Louisiana | Catahoula Parish, Louisiana | 0.980 |
| 211 | Elk County, Kansas | Wilson County, Kansas | 0.980 |
| 212 | Iron County, Missouri | Reynolds County, Missouri | 0.980 |
| 213 | Pottawattamie County, Iowa | Shelby County, Iowa | 0.980 |
| 214 | Brazos County, Texas | Leon County, Texas | 0.979 |
| 215 | Dooly County, Georgia | Sumter County, Georgia | 0.979 |
| 216 | Mingo County, West Virginia | Wayne County, West Virginia | 0.979 |
| 217 | Cedar County, Nebraska | Clay County, South Dakota | 0.979 |
| 218 | Levy County, Florida | Marion County, Florida | 0.979 |
| 219 | Hernando County, Florida | Sumter County, Florida | 0.978 |
| 220 | Franklin County, Tennessee | Marion County, Tennessee | 0.978 |
| 221 | Bronx County, New York | Westchester County, New York | 0.977 |
| 222 | Union County, Illinois | Perry County, Missouri | 0.977 |
| 223 | Bullock County, Alabama | Russell County, Alabama | 0.977 |
| 224 | Sheridan County, Montana | Williams County, North Dakota | 0.976 |
| 225 | Scotland County, North Carolina | Marlboro County, South Carolina | 0.976 |
| 226 | Issaquena County, Mississippi | Yazoo County, Mississippi | 0.976 |
| 227 | Lincoln County, Georgia | McCormick County, South Carolina | 0.976 |
| 228 | Elko County, Nevada | Box Elder County, Utah | 0.976 |
| 229 | Adair County, Kentucky | Casey County, Kentucky | 0.976 |
| 230 | Fannin County, Georgia | Polk County, Tennessee | 0.975 |
| 231 | Bee County, Texas | San Patricio County, Texas | 0.975 |
| 232 | Powell County, Kentucky | Wolfe County, Kentucky | 0.975 |
| 233 | Dent County, Missouri | Iron County, Missouri | 0.975 |
| 234 | Harlan County, Kentucky | Lee County, Virginia | 0.975 |
| 235 | Elliott County, Kentucky | Lawrence County, Kentucky | 0.975 |

| | | | |
|-----|---------------------------------|------------------------------------|-------|
| 236 | Nemaha County, Kansas | Pottawatomie County, Kansas | 0.974 |
| 237 | Flagler County, Florida | Putnam County, Florida | 0.974 |
| 238 | Jennings County, Indiana | Scott County, Indiana | 0.974 |
| 239 | Monroe County, Illinois | Jefferson County, Missouri | 0.974 |
| 240 | Clay County, Mississippi | Webster County, Mississippi | 0.973 |
| 241 | McCreary County, Kentucky | Campbell County, Tennessee | 0.973 |
| 242 | Pennington County, South Dakota | Ziebach County, South Dakota | 0.973 |
| 243 | Bergen County, New Jersey | Bronx County, New York | 0.973 |
| 244 | Franklin County, Tennessee | Moore County, Tennessee | 0.972 |
| 245 | Roger Mills County, Oklahoma | Wheeler County, Texas | 0.972 |
| 246 | Carter County, Kentucky | Lawrence County, Kentucky | 0.972 |
| 247 | Davis County, Iowa | Monroe County, Iowa | 0.972 |
| 248 | Pope County, Illinois | Saline County, Illinois | 0.972 |
| 249 | La Paz County, Arizona | San Bernardino County, California | 0.972 |
| 250 | Lincoln County, West Virginia | Putnam County, West Virginia | 0.972 |
| 251 | Benton County, Arkansas | McDonald County, Missouri | 0.972 |
| 252 | Alexander County, Illinois | Cape Girardeau County, Missouri | 0.971 |
| 253 | Polk County, Texas | Tyler County, Texas | 0.971 |
| 254 | Jackson County, Alabama | Franklin County, Tennessee | 0.971 |
| 255 | Humboldt County, Nevada | Malheur County, Oregon | 0.971 |
| 256 | Adams County, Wisconsin | Wood County, Wisconsin | 0.971 |
| 257 | Chester County, Tennessee | McNairy County, Tennessee | 0.971 |
| 258 | Mono County, California | Lyon County, Nevada | 0.970 |
| 259 | Dooly County, Georgia | Wilcox County, Georgia | 0.970 |
| 260 | Dewey County, Oklahoma | Woodward County, Oklahoma | 0.970 |
| 261 | Spencer County, Indiana | Daviess County, Kentucky | 0.970 |
| 262 | Corson County, South Dakota | Dewey County, South Dakota | 0.970 |
| 263 | Wibaux County, Montana | Golden Valley County, North Dakota | 0.970 |
| 264 | Coconino County, Arizona | Mohave County, Arizona | 0.969 |
| 265 | Sierra County, California | Yuba County, California | 0.969 |
| 266 | Loving County, Texas | Reeves County, Texas | 0.969 |
| 267 | Citrus County, Florida | Levy County, Florida | 0.969 |
| 268 | Bracken County, Kentucky | Harrison County, Kentucky | 0.969 |
| 269 | Highlands County, Florida | Okeechobee County, Florida | 0.969 |
| 270 | Cassia County, Idaho | Elko County, Nevada | 0.968 |
| 271 | Hartley County, Texas | Sherman County, Texas | 0.968 |
| 272 | Bryan County, Georgia | Liberty County, Georgia | 0.967 |
| 273 | Hardin County, Illinois | Livingston County, Kentucky | 0.967 |

| | | | |
|-----|---------------------------------|----------------------------------|-------|
| 274 | Pike County, Kentucky | Dickenson County, Virginia | 0.967 |
| 275 | Somerset County, Maryland | Accomack County, Virginia | 0.967 |
| 276 | Plaquemines Parish, Louisiana | Saint Bernard Parish, Louisiana | 0.967 |
| 277 | Dillon County, South Carolina | Marlboro County, South Carolina | 0.967 |
| 278 | Grant Parish, Louisiana | Rapides Parish, Louisiana | 0.966 |
| 279 | Oktibbeha County, Mississippi | Webster County, Mississippi | 0.966 |
| 280 | Coleman County, Texas | Concho County, Texas | 0.966 |
| 281 | Alcorn County, Mississippi | Tippah County, Mississippi | 0.965 |
| 282 | Rockingham County, Virginia | Pendleton County, West Virginia | 0.965 |
| 283 | Daviess County, Missouri | DeKalb County, Missouri | 0.965 |
| 284 | Mercer County, Kentucky | Washington County, Kentucky | 0.965 |
| 285 | Cape Girardeau County, Missouri | Scott County, Missouri | 0.965 |
| 286 | Callahan County, Texas | Jones County, Texas | 0.965 |
| 287 | Rapides Parish, Louisiana | Vernon Parish, Louisiana | 0.965 |
| 288 | Harris County, Texas | Liberty County, Texas | 0.965 |
| 289 | Crowley County, Colorado | El Paso County, Colorado | 0.965 |
| 290 | McDuffie County, Georgia | Taliaferro County, Georgia | 0.964 |
| 291 | Fleming County, Kentucky | Nicholas County, Kentucky | 0.964 |
| 292 | Clinch County, Georgia | Ware County, Georgia | 0.964 |
| 293 | Van Buren County, Tennessee | Warren County, Tennessee | 0.964 |
| 294 | Baca County, Colorado | Las Animas County, Colorado | 0.964 |
| 295 | Gloucester County, Virginia | Mathews County, Virginia | 0.964 |
| 296 | Brown County, Illinois | Schuyler County, Illinois | 0.963 |
| 297 | Bryan County, Georgia | Bulloch County, Georgia | 0.963 |
| 298 | Sioux County, Nebraska | Fall River County, South Dakota | 0.963 |
| 299 | Clinch County, Georgia | Echols County, Georgia | 0.963 |
| 300 | Adams County, Indiana | Jay County, Indiana | 0.963 |
| 301 | Charles County, Maryland | Prince George's County, Maryland | 0.963 |
| 302 | Bacon County, Georgia | Ware County, Georgia | 0.963 |
| 303 | Carson County, Texas | Donley County, Texas | 0.962 |
| 304 | Desha County, Arkansas | Phillips County, Arkansas | 0.962 |
| 305 | Bullock County, Alabama | Pike County, Alabama | 0.962 |
| 306 | Grant County, West Virginia | Hampshire County, West Virginia | 0.962 |
| 307 | Clay County, Kentucky | Laurel County, Kentucky | 0.962 |
| 308 | Haywood County, North Carolina | Cocke County, Tennessee | 0.962 |
| 309 | Franklin County, Alabama | Marion County, Alabama | 0.962 |
| 310 | Lyon County, Iowa | Minnehaha County, South Dakota | 0.961 |
| 311 | Angelina County, Texas | Trinity County, Texas | 0.961 |

| | | | |
|-----|-------------------------------|------------------------------------|-------|
| 312 | Banks County, Georgia | Jackson County, Georgia | 0.961 |
| 313 | Green County, Kentucky | Hart County, Kentucky | 0.961 |
| 314 | Dubois County, Indiana | Orange County, Indiana | 0.961 |
| 315 | Pike County, Georgia | Upson County, Georgia | 0.961 |
| 316 | White County, Illinois | Gibson County, Indiana | 0.961 |
| 317 | Marion County, Alabama | Walker County, Alabama | 0.960 |
| 318 | Butts County, Georgia | Monroe County, Georgia | 0.960 |
| 319 | Cumberland County, Tennessee | Morgan County, Tennessee | 0.960 |
| 320 | Bryan County, Georgia | Evans County, Georgia | 0.960 |
| 321 | Alachua County, Florida | Marion County, Florida | 0.960 |
| 322 | Nye County, Nevada | White Pine County, Nevada | 0.960 |
| 323 | Clay County, Georgia | Quitman County, Georgia | 0.960 |
| 324 | Grenada County, Mississippi | Tallahatchie County, Mississippi | 0.960 |
| 325 | Jones County, Texas | Shackelford County, Texas | 0.960 |
| 326 | Juniata County, Pennsylvania | Perry County, Pennsylvania | 0.960 |
| 327 | Fleming County, Kentucky | Mason County, Kentucky | 0.960 |
| 328 | Miami-Dade County, Florida | Monroe County, Florida | 0.959 |
| 329 | Clay County, Kansas | Geary County, Kansas | 0.959 |
| 330 | Cleveland County, Arkansas | Lincoln County, Arkansas | 0.958 |
| 331 | Carroll County, Tennessee | Madison County, Tennessee | 0.958 |
| 332 | Barbour County, West Virginia | Harrison County, West Virginia | 0.957 |
| 333 | Bourbon County, Kentucky | Nicholas County, Kentucky | 0.957 |
| 334 | Chicot County, Arkansas | Issaquena County, Mississippi | 0.957 |
| 335 | Page County, Virginia | Warren County, Virginia | 0.957 |
| 336 | Sioux County, Iowa | Union County, South Dakota | 0.957 |
| 337 | Fallon County, Montana | Golden Valley County, North Dakota | 0.957 |
| 338 | San Augustine County, Texas | Shelby County, Texas | 0.956 |
| 339 | Henderson County, Kentucky | McLean County, Kentucky | 0.956 |
| 340 | Catron County, New Mexico | Sierra County, New Mexico | 0.956 |
| 341 | Orleans Parish, Louisiana | Saint Bernard Parish, Louisiana | 0.956 |
| 342 | Bledsoe County, Tennessee | Rhea County, Tennessee | 0.956 |
| 343 | Brown County, South Dakota | McPherson County, South Dakota | 0.956 |
| 344 | Hamilton County, Tennessee | Marion County, Tennessee | 0.956 |
| 345 | Kemper County, Mississippi | Newton County, Mississippi | 0.955 |
| 346 | Benson County, North Dakota | Towner County, North Dakota | 0.955 |
| 347 | Montrose County, Colorado | San Juan County, Utah | 0.955 |
| 348 | Catoosa County, Georgia | Walker County, Georgia | 0.955 |
| 349 | Baca County, Colorado | Bent County, Colorado | 0.955 |

| | | | |
|-----|--------------------------------|-----------------------------------|-------|
| 350 | Harrison County, Kentucky | Nicholas County, Kentucky | 0.954 |
| 351 | Emery County, Utah | Grand County, Utah | 0.954 |
| 352 | Fallon County, Montana | Slope County, North Dakota | 0.954 |
| 353 | Athens County, Ohio | Morgan County, Ohio | 0.953 |
| 354 | Dodge County, Georgia | Pulaski County, Georgia | 0.953 |
| 355 | Lea County, New Mexico | Loving County, Texas | 0.953 |
| 356 | Giles County, Virginia | Summers County, West Virginia | 0.952 |
| 357 | Kiowa County, Colorado | Otero County, Colorado | 0.952 |
| 358 | Douglas County, Missouri | Howell County, Missouri | 0.952 |
| 359 | Ashland County, Ohio | Holmes County, Ohio | 0.952 |
| 360 | Butler County, Kansas | Marion County, Kansas | 0.951 |
| 361 | Cabell County, West Virginia | Lincoln County, West Virginia | 0.951 |
| 362 | Houston County, Georgia | Peach County, Georgia | 0.951 |
| 363 | Chambers County, Alabama | Randolph County, Alabama | 0.951 |
| 364 | Toombs County, Georgia | Treutlen County, Georgia | 0.951 |
| 365 | De Soto Parish, Louisiana | Shelby County, Texas | 0.951 |
| 366 | Hickman County, Tennessee | Maury County, Tennessee | 0.951 |
| 367 | Crawford County, Indiana | Dubois County, Indiana | 0.951 |
| 368 | Barber County, Kansas | Kingman County, Kansas | 0.951 |
| 369 | Cross County, Arkansas | Saint Francis County, Arkansas | 0.950 |
| 370 | DeKalb County, Alabama | Dade County, Georgia | 0.950 |
| 371 | Montgomery County, Arkansas | Yell County, Arkansas | 0.950 |
| 372 | Collier County, Florida | Monroe County, Florida | 0.950 |
| 373 | Shannon County, Missouri | Texas County, Missouri | 0.950 |
| 374 | Crawford County, Missouri | Iron County, Missouri | 0.949 |
| 375 | Howard County, Arkansas | Montgomery County, Arkansas | 0.949 |
| 376 | Jackson County, Georgia | Oconee County, Georgia | 0.949 |
| 377 | Benton County, Missouri | Hickory County, Missouri | 0.949 |
| 378 | Trinity County, Texas | Walker County, Texas | 0.949 |
| 379 | Estill County, Kentucky | Madison County, Kentucky | 0.949 |
| 380 | Latah County, Idaho | Shoshone County, Idaho | 0.949 |
| 381 | Saint Francis County, Arkansas | Woodruff County, Arkansas | 0.948 |
| 382 | Monroe County, Tennessee | Polk County, Tennessee | 0.948 |
| 383 | Jefferson County, Montana | Madison County, Montana | 0.948 |
| 384 | Sutton County, Texas | Val Verde County, Texas | 0.948 |
| 385 | Chattahoochee County, Georgia | Muscogee County, Georgia | 0.948 |
| 386 | Green County, Kentucky | Metcalfe County, Kentucky | 0.948 |
| 387 | Allen Parish, Louisiana | Jefferson Davis Parish, Louisiana | 0.948 |

| | | | |
|-----|--------------------------------|----------------------------------|-------|
| 388 | Caldwell County, Missouri | DeKalb County, Missouri | 0.948 |
| 389 | Camas County, Idaho | Elmore County, Idaho | 0.948 |
| 390 | Henry County, Missouri | Johnson County, Missouri | 0.947 |
| 391 | Drew County, Arkansas | Lincoln County, Arkansas | 0.946 |
| 392 | Hart County, Georgia | Madison County, Georgia | 0.946 |
| 393 | Cumberland County, Tennessee | Putnam County, Tennessee | 0.946 |
| 394 | Appanoose County, Iowa | Monroe County, Iowa | 0.946 |
| 395 | Guernsey County, Ohio | Tuscarawas County, Ohio | 0.946 |
| 396 | McKinley County, New Mexico | San Juan County, New Mexico | 0.945 |
| 397 | Estill County, Kentucky | Lee County, Kentucky | 0.945 |
| 398 | McDowell County, West Virginia | Mercer County, West Virginia | 0.945 |
| 399 | Caldwell Parish, Louisiana | Winn Parish, Louisiana | 0.945 |
| 400 | Wayne County, Indiana | Darke County, Ohio | 0.945 |
| 401 | Allen County, Kentucky | Macon County, Tennessee | 0.944 |
| 402 | Jackson County, Arkansas | Poinsett County, Arkansas | 0.944 |
| 403 | Chester County, Tennessee | Henderson County, Tennessee | 0.944 |
| 404 | Barbour County, Alabama | Bullock County, Alabama | 0.944 |
| 405 | Putnam County, Florida | Volusia County, Florida | 0.944 |
| 406 | Daniels County, Montana | Valley County, Montana | 0.944 |
| 407 | Atoka County, Oklahoma | Choctaw County, Oklahoma | 0.944 |
| 408 | Gilmer County, West Virginia | Lewis County, West Virginia | 0.943 |
| 409 | Montgomery County, Mississippi | Webster County, Mississippi | 0.943 |
| 410 | Catahoula Parish, Louisiana | Franklin Parish, Louisiana | 0.943 |
| 411 | Apache County, Arizona | Graham County, Arizona | 0.943 |
| 412 | Clinton County, Pennsylvania | Union County, Pennsylvania | 0.943 |
| 413 | Emanuel County, Georgia | Toombs County, Georgia | 0.943 |
| 414 | Cibola County, New Mexico | McKinley County, New Mexico | 0.943 |
| 415 | Pope County, Arkansas | Van Buren County, Arkansas | 0.942 |
| 416 | Claiborne Parish, Louisiana | Webster Parish, Louisiana | 0.942 |
| 417 | Churchill County, Nevada | Pershing County, Nevada | 0.942 |
| 418 | Preston County, West Virginia | Taylor County, West Virginia | 0.942 |
| 419 | Menifee County, Kentucky | Wolfe County, Kentucky | 0.942 |
| 420 | Humboldt County, Nevada | Pershing County, Nevada | 0.942 |
| 421 | Hamilton County, Texas | Lampasas County, Texas | 0.942 |
| 422 | Paulding County, Georgia | Polk County, Georgia | 0.942 |
| 423 | Crisp County, Georgia | Dooly County, Georgia | 0.942 |
| 424 | Marion County, Kentucky | Nelson County, Kentucky | 0.941 |
| 425 | Elbert County, Georgia | McCormick County, South Carolina | 0.941 |

| | | | |
|-----|-------------------------------|----------------------------------|-------|
| 426 | Humboldt County, Nevada | Harney County, Oregon | 0.941 |
| 427 | Liberty County, Montana | Toole County, Montana | 0.941 |
| 428 | Bastrop County, Texas | Fayette County, Texas | 0.941 |
| 429 | Banks County, Georgia | Madison County, Georgia | 0.941 |
| 430 | Franklin County, Illinois | Jackson County, Illinois | 0.941 |
| 431 | Baker County, Florida | Charlton County, Georgia | 0.940 |
| 432 | Lee County, Virginia | Scott County, Virginia | 0.940 |
| 433 | Grant County, West Virginia | Randolph County, West Virginia | 0.940 |
| 434 | Big Horn County, Montana | Treasure County, Montana | 0.940 |
| 435 | Bowman County, North Dakota | Slope County, North Dakota | 0.939 |
| 436 | McDonald County, Missouri | Delaware County, Oklahoma | 0.939 |
| 437 | Lawrence County, Kentucky | Morgan County, Kentucky | 0.939 |
| 438 | Franklin County, Missouri | Washington County, Missouri | 0.938 |
| 439 | Lassen County, California | Shasta County, California | 0.938 |
| 440 | Grant County, West Virginia | Mineral County, West Virginia | 0.938 |
| 441 | Emanuel County, Georgia | Johnson County, Georgia | 0.938 |
| 442 | Nueces County, Texas | San Patricio County, Texas | 0.938 |
| 443 | Liberty County, Montana | Pondera County, Montana | 0.937 |
| 444 | Adams County, Ohio | Highland County, Ohio | 0.937 |
| 445 | Fannin County, Georgia | Murray County, Georgia | 0.937 |
| 446 | Boyle County, Kentucky | Washington County, Kentucky | 0.937 |
| 447 | Adams County, Wisconsin | Portage County, Wisconsin | 0.936 |
| 448 | Decatur County, Indiana | Jennings County, Indiana | 0.936 |
| 449 | Caddo Parish, Louisiana | Marion County, Texas | 0.936 |
| 450 | Anne Arundel County, Maryland | Prince George's County, Maryland | 0.936 |
| 451 | Cass County, Missouri | Henry County, Missouri | 0.936 |
| 452 | Eastland County, Texas | Erath County, Texas | 0.936 |
| 453 | Lafayette County, Mississippi | Yalobusha County, Mississippi | 0.936 |
| 454 | Quitman County, Georgia | Randolph County, Georgia | 0.935 |
| 455 | Mississippi County, Arkansas | Poinsett County, Arkansas | 0.935 |
| 456 | Itawamba County, Mississippi | Prentiss County, Mississippi | 0.935 |
| 457 | Crawford County, Georgia | Peach County, Georgia | 0.935 |
| 458 | La Paz County, Arizona | Riverside County, California | 0.934 |
| 459 | Leon County, Texas | Madison County, Texas | 0.934 |
| 460 | Anderson County, Texas | Henderson County, Texas | 0.934 |
| 461 | Claiborne County, Tennessee | Hancock County, Tennessee | 0.934 |
| 462 | George County, Mississippi | Greene County, Mississippi | 0.933 |
| 463 | Raleigh County, West Virginia | Wyoming County, West Virginia | 0.933 |

| | | | |
|-----|-------------------------------|----------------------------------|-------|
| 464 | Marion County, Georgia | Talbot County, Georgia | 0.933 |
| 465 | Jackson County, Kansas | Nemaha County, Kansas | 0.933 |
| 466 | Columbia County, Arkansas | Claiborne Parish, Louisiana | 0.932 |
| 467 | Bland County, Virginia | Smyth County, Virginia | 0.932 |
| 468 | Armstrong County, Texas | Donley County, Texas | 0.932 |
| 469 | Butler County, Alabama | Covington County, Alabama | 0.932 |
| 470 | Jim Wells County, Texas | San Patricio County, Texas | 0.932 |
| 471 | Lincoln County, Nevada | Nye County, Nevada | 0.932 |
| 472 | Campbell County, South Dakota | Walworth County, South Dakota | 0.931 |
| 473 | Nevada County, California | Yuba County, California | 0.931 |
| 474 | Price County, Wisconsin | Taylor County, Wisconsin | 0.931 |
| 475 | Laclede County, Missouri | Pulaski County, Missouri | 0.931 |
| 476 | Anderson County, Tennessee | Campbell County, Tennessee | 0.931 |
| 477 | Bibb County, Georgia | Peach County, Georgia | 0.931 |
| 478 | Clay County, West Virginia | Roane County, West Virginia | 0.930 |
| 479 | Jackson Parish, Louisiana | Ouachita Parish, Louisiana | 0.930 |
| 480 | Hamblen County, Tennessee | Jefferson County, Tennessee | 0.929 |
| 481 | Jackson Parish, Louisiana | Lincoln Parish, Louisiana | 0.929 |
| 482 | Lincoln County, Nevada | Millard County, Utah | 0.929 |
| 483 | Hardeman County, Tennessee | McNairy County, Tennessee | 0.929 |
| 484 | Rankin County, Mississippi | Smith County, Mississippi | 0.929 |
| 485 | Fulton County, Indiana | Wabash County, Indiana | 0.929 |
| 486 | Carroll County, Missouri | Ray County, Missouri | 0.929 |
| 487 | Cooper County, Missouri | Pettis County, Missouri | 0.929 |
| 488 | Henderson County, Tennessee | Madison County, Tennessee | 0.929 |
| 489 | Bledsoe County, Tennessee | Sequatchie County, Tennessee | 0.929 |
| 490 | Grand County, Utah | Wayne County, Utah | 0.929 |
| 491 | Kanawha County, West Virginia | Lincoln County, West Virginia | 0.929 |
| 492 | Columbia County, Georgia | Edgefield County, South Carolina | 0.929 |
| 493 | Floyd County, Kentucky | Pike County, Kentucky | 0.928 |
| 494 | Ben Hill County, Georgia | Turner County, Georgia | 0.928 |
| 495 | Cherokee County, Georgia | Gordon County, Georgia | 0.928 |
| 496 | Itawamba County, Mississippi | Monroe County, Mississippi | 0.928 |
| 497 | Randolph County, Alabama | Carroll County, Georgia | 0.928 |
| 498 | Gallatin County, Montana | Jefferson County, Montana | 0.928 |
| 499 | Hancock County, Mississippi | Harrison County, Mississippi | 0.928 |
| 500 | Calhoun County, Mississippi | Yalobusha County, Mississippi | 0.928 |
| 501 | Douglas County, Missouri | Ozark County, Missouri | 0.928 |

| | | | |
|-----|----------------------------------|--------------------------------|-------|
| 502 | Surry County, North Carolina | Patrick County, Virginia | 0.928 |
| 503 | Kootenai County, Idaho | Shoshone County, Idaho | 0.928 |
| 504 | Howell County, Missouri | Texas County, Missouri | 0.927 |
| 505 | Elbert County, Georgia | Madison County, Georgia | 0.927 |
| 506 | Henry County, Kentucky | Shelby County, Kentucky | 0.927 |
| 507 | Cowley County, Kansas | Elk County, Kansas | 0.927 |
| 508 | Franklin County, Illinois | Jefferson County, Illinois | 0.927 |
| 509 | Duplin County, North Carolina | Onslow County, North Carolina | 0.927 |
| 510 | Richland County, Montana | McKenzie County, North Dakota | 0.926 |
| 511 | Bledsoe County, Tennessee | White County, Tennessee | 0.926 |
| 512 | Jefferson County, Oregon | Linn County, Oregon | 0.926 |
| 513 | Russell County, Virginia | Wise County, Virginia | 0.926 |
| 514 | Grant County, Kentucky | Harrison County, Kentucky | 0.926 |
| 515 | Sequatchie County, Tennessee | Van Buren County, Tennessee | 0.926 |
| 516 | East Feliciana Parish, Louisiana | Saint Helena Parish, Louisiana | 0.925 |
| 517 | Rock County, Minnesota | Minnehaha County, South Dakota | 0.925 |
| 518 | Lea County, New Mexico | Andrews County, Texas | 0.925 |
| 519 | Attala County, Mississippi | Leake County, Mississippi | 0.925 |
| 520 | Shoshone County, Idaho | Sanders County, Montana | 0.925 |
| 521 | Christian County, Kentucky | Muhlenberg County, Kentucky | 0.925 |
| 522 | Holmes County, Ohio | Wayne County, Ohio | 0.925 |
| 523 | Monroe County, Ohio | Tyler County, West Virginia | 0.925 |
| 524 | Smyth County, Virginia | Wythe County, Virginia | 0.925 |
| 525 | Searcy County, Arkansas | Van Buren County, Arkansas | 0.925 |
| 526 | Atoka County, Oklahoma | Pushmataha County, Oklahoma | 0.924 |
| 527 | Houston County, Georgia | Pulaski County, Georgia | 0.924 |
| 528 | Marshall County, Kansas | Pottawatomie County, Kansas | 0.924 |
| 529 | Cooper County, Missouri | Morgan County, Missouri | 0.924 |
| 530 | Fentress County, Tennessee | Pickett County, Tennessee | 0.923 |
| 531 | Van Buren County, Tennessee | White County, Tennessee | 0.923 |
| 532 | Gadsden County, Florida | Decatur County, Georgia | 0.922 |
| 533 | Adams County, Indiana | Allen County, Indiana | 0.922 |
| 534 | Davis County, Iowa | Scotland County, Missouri | 0.922 |
| 535 | Christian County, Illinois | Shelby County, Illinois | 0.922 |
| 536 | Buchanan County, Virginia | McDowell County, West Virginia | 0.922 |
| 537 | Delaware County, Iowa | Dubuque County, Iowa | 0.922 |
| 538 | Garrard County, Kentucky | Lincoln County, Kentucky | 0.922 |
| 539 | Attala County, Mississippi | Choctaw County, Mississippi | 0.921 |

| | | | |
|-----|--------------------------------|----------------------------------|-------|
| 540 | Barrow County, Georgia | Gwinnett County, Georgia | 0.921 |
| 541 | McMinn County, Tennessee | Polk County, Tennessee | 0.921 |
| 542 | Menominee County, Wisconsin | Shawano County, Wisconsin | 0.921 |
| 543 | Gratiot County, Michigan | Isabella County, Michigan | 0.921 |
| 544 | McIntosh County, Georgia | Wayne County, Georgia | 0.920 |
| 545 | Johnson County, Illinois | Saline County, Illinois | 0.920 |
| 546 | Logan County, Colorado | Kimball County, Nebraska | 0.920 |
| 547 | Fulton County, Kentucky | Weakley County, Tennessee | 0.920 |
| 548 | Perkins County, South Dakota | Ziebach County, South Dakota | 0.919 |
| 549 | Scott County, Minnesota | Sibley County, Minnesota | 0.919 |
| 550 | Roosevelt County, New Mexico | Cochran County, Texas | 0.919 |
| 551 | Bollinger County, Missouri | Madison County, Missouri | 0.919 |
| 552 | Concho County, Texas | Runnels County, Texas | 0.919 |
| 553 | Harrison County, Ohio | Tuscarawas County, Ohio | 0.918 |
| 554 | McPherson County, South Dakota | Walworth County, South Dakota | 0.918 |
| 555 | Clay County, Alabama | Cleburne County, Alabama | 0.917 |
| 556 | Calvert County, Maryland | Prince George's County, Maryland | 0.917 |
| 557 | Falls County, Texas | Limestone County, Texas | 0.917 |
| 558 | Long County, Georgia | McIntosh County, Georgia | 0.916 |
| 559 | Conway County, Arkansas | Yell County, Arkansas | 0.916 |
| 560 | Ben Hill County, Georgia | Telfair County, Georgia | 0.916 |
| 561 | Chattahoochee County, Georgia | Talbot County, Georgia | 0.916 |
| 562 | Garrard County, Kentucky | Rockcastle County, Kentucky | 0.916 |
| 563 | Carroll County, Mississippi | Holmes County, Mississippi | 0.915 |
| 564 | Miller County, Missouri | Osage County, Missouri | 0.915 |
| 565 | Buchanan County, Missouri | DeKalb County, Missouri | 0.914 |
| 566 | Irion County, Texas | Tom Green County, Texas | 0.914 |
| 567 | Hickman County, Kentucky | Obion County, Tennessee | 0.914 |
| 568 | Okeechobee County, Florida | Osceola County, Florida | 0.913 |
| 569 | Spencer County, Indiana | Hancock County, Kentucky | 0.913 |
| 570 | Montgomery County, Iowa | Pottawattamie County, Iowa | 0.913 |
| 571 | Cooke County, Texas | Montague County, Texas | 0.913 |
| 572 | Floyd County, Georgia | Polk County, Georgia | 0.913 |
| 573 | Carter County, Missouri | Shannon County, Missouri | 0.912 |
| 574 | Cullman County, Alabama | Walker County, Alabama | 0.912 |
| 575 | Cedar County, Iowa | Scott County, Iowa | 0.912 |
| 576 | Dewey County, Oklahoma | Roger Mills County, Oklahoma | 0.912 |
| 577 | Oldham County, Kentucky | Trimble County, Kentucky | 0.912 |

| | | | |
|-----|--------------------------------|----------------------------------|-------|
| 578 | Bell County, Texas | Lampasas County, Texas | 0.912 |
| 579 | Montezuma County, Colorado | San Juan County, New Mexico | 0.911 |
| 580 | Jasper County, Iowa | Tama County, Iowa | 0.911 |
| 581 | Grant County, Indiana | Wells County, Indiana | 0.911 |
| 582 | Claiborne Parish, Louisiana | Union Parish, Louisiana | 0.911 |
| 583 | Harlan County, Kentucky | Perry County, Kentucky | 0.910 |
| 584 | Meriwether County, Georgia | Talbot County, Georgia | 0.910 |
| 585 | Daviess County, Missouri | Gentry County, Missouri | 0.910 |
| 586 | Reeves County, Texas | Ward County, Texas | 0.910 |
| 587 | Marshall County, Iowa | Tama County, Iowa | 0.910 |
| 588 | Catahoula Parish, Louisiana | Tensas Parish, Louisiana | 0.910 |
| 589 | Bollinger County, Missouri | Wayne County, Missouri | 0.909 |
| 590 | Kiowa County, Colorado | Lincoln County, Colorado | 0.909 |
| 591 | Fayette County, Alabama | Walker County, Alabama | 0.909 |
| 592 | Boone County, West Virginia | Wyoming County, West Virginia | 0.909 |
| 593 | Brown County, Indiana | Jackson County, Indiana | 0.909 |
| 594 | Scott County, Virginia | Wise County, Virginia | 0.909 |
| 595 | Crockett County, Tennessee | Dyer County, Tennessee | 0.909 |
| 596 | Atkinson County, Georgia | Coffee County, Georgia | 0.909 |
| 597 | Essex County, Virginia | Richmond County, Virginia | 0.909 |
| 598 | Rockingham County, Virginia | Hardy County, West Virginia | 0.908 |
| 599 | Catahoula Parish, Louisiana | Concordia Parish, Louisiana | 0.908 |
| 600 | Jackson County, Illinois | Williamson County, Illinois | 0.908 |
| 601 | Burt County, Nebraska | Thurston County, Nebraska | 0.908 |
| 602 | Columbia County, Georgia | McCormick County, South Carolina | 0.908 |
| 603 | Maries County, Missouri | Osage County, Missouri | 0.908 |
| 604 | Effingham County, Georgia | Hampton County, South Carolina | 0.907 |
| 605 | Screven County, Georgia | Allendale County, South Carolina | 0.907 |
| 606 | Treutlen County, Georgia | Wheeler County, Georgia | 0.907 |
| 607 | Hardin County, Illinois | Crittenden County, Kentucky | 0.907 |
| 608 | Fulton County, New York | Hamilton County, New York | 0.907 |
| 609 | Fayette County, Tennessee | Tipton County, Tennessee | 0.906 |
| 610 | Madison County, North Carolina | Cocke County, Tennessee | 0.906 |
| 611 | Hardin County, Texas | Polk County, Texas | 0.906 |
| 612 | Hartley County, Texas | Potter County, Texas | 0.906 |
| 613 | Wibaux County, Montana | McKenzie County, North Dakota | 0.906 |
| 614 | Benson County, North Dakota | Eddy County, North Dakota | 0.906 |
| 615 | Hamilton County, New York | Herkimer County, New York | 0.906 |

| | | | |
|-----|--------------------------------|---------------------------------|-------|
| 616 | Crittenden County, Arkansas | Saint Francis County, Arkansas | 0.906 |
| 617 | Briscoe County, Texas | Swisher County, Texas | 0.905 |
| 618 | Grant County, West Virginia | Tucker County, West Virginia | 0.905 |
| 619 | Grant County, Arkansas | Saline County, Arkansas | 0.905 |
| 620 | Lassen County, California | Plumas County, California | 0.905 |
| 621 | Appling County, Georgia | Bacon County, Georgia | 0.904 |
| 622 | Frio County, Texas | Uvalde County, Texas | 0.904 |
| 623 | Union County, Illinois | Cape Girardeau County, Missouri | 0.904 |
| 624 | Fayette County, West Virginia | Summers County, West Virginia | 0.904 |
| 625 | Bracken County, Kentucky | Clermont County, Ohio | 0.903 |
| 626 | Lee County, Arkansas | Phillips County, Arkansas | 0.903 |
| 627 | Richmond County, Virginia | Westmoreland County, Virginia | 0.903 |
| 628 | Pike County, Georgia | Spalding County, Georgia | 0.903 |
| 629 | Pecos County, Texas | Ward County, Texas | 0.903 |
| 630 | Amelia County, Virginia | Cumberland County, Virginia | 0.902 |
| 631 | Cumberland County, Tennessee | Roane County, Tennessee | 0.902 |
| 632 | Grenada County, Mississippi | Leflore County, Mississippi | 0.902 |
| 633 | Dixon County, Nebraska | Clay County, South Dakota | 0.902 |
| 634 | Natchitoches Parish, Louisiana | Red River Parish, Louisiana | 0.902 |
| 635 | Mono County, California | Mineral County, Nevada | 0.902 |
| 636 | Baker County, Georgia | Miller County, Georgia | 0.901 |
| 637 | Buchanan County, Iowa | Delaware County, Iowa | 0.901 |
| 638 | Lafayette County, Arkansas | Caddo Parish, Louisiana | 0.901 |
| 639 | Brown County, Illinois | Morgan County, Illinois | 0.901 |
| 640 | Lake County, Montana | Missoula County, Montana | 0.901 |
| 641 | Carroll County, Arkansas | Newton County, Arkansas | 0.901 |
| 642 | Roosevelt County, Montana | Sheridan County, Montana | 0.900 |
| 643 | Dallam County, Texas | Hartley County, Texas | 0.900 |
| 644 | Lassen County, California | Washoe County, Nevada | 0.900 |
| 645 | Rusk County, Wisconsin | Taylor County, Wisconsin | 0.900 |
| 646 | Conway County, Arkansas | Pope County, Arkansas | 0.899 |
| 647 | Putnam County, New York | Rockland County, New York | 0.899 |
| 648 | Franklin County, Indiana | Ripley County, Indiana | 0.899 |
| 649 | Briscoe County, Texas | Donley County, Texas | 0.899 |
| 650 | Bonner County, Idaho | Shoshone County, Idaho | 0.899 |
| 651 | Beaver County, Oklahoma | Lipscomb County, Texas | 0.899 |
| 652 | Baker County, Georgia | Calhoun County, Georgia | 0.899 |
| 653 | Carroll County, Indiana | White County, Indiana | 0.899 |

| | | | |
|-----|------------------------------------|-----------------------------------|-------|
| 654 | Hart County, Kentucky | Larue County, Kentucky | 0.899 |
| 655 | Jackson County, Missouri | Ray County, Missouri | 0.899 |
| 656 | Jasper County, Indiana | Lake County, Indiana | 0.898 |
| 657 | Desha County, Arkansas | Bolivar County, Mississippi | 0.898 |
| 658 | Carter County, Montana | Custer County, Montana | 0.897 |
| 659 | Ozark County, Missouri | Taney County, Missouri | 0.897 |
| 660 | Cecil County, Maryland | Lancaster County, Pennsylvania | 0.897 |
| 661 | Wallowa County, Oregon | Columbia County, Washington | 0.897 |
| 662 | Camden County, North Carolina | Currituck County, North Carolina | 0.897 |
| 663 | Bracken County, Kentucky | Pendleton County, Kentucky | 0.897 |
| 664 | Bennett County, South Dakota | Jackson County, South Dakota | 0.896 |
| 665 | East Baton Rouge Parish, Louisiana | East Feliciana Parish, Louisiana | 0.896 |
| 666 | Douglas County, Colorado | Teller County, Colorado | 0.896 |
| 667 | Owyhee County, Idaho | Humboldt County, Nevada | 0.896 |
| 668 | Columbia County, Oregon | Wahkiakum County, Washington | 0.894 |
| 669 | Jefferson County, Oregon | Marion County, Oregon | 0.894 |
| 670 | Rankin County, Mississippi | Scott County, Mississippi | 0.894 |
| 671 | Overton County, Tennessee | Pickett County, Tennessee | 0.894 |
| 672 | Mississippi County, Arkansas | Dunklin County, Missouri | 0.893 |
| 673 | Paulding County, Ohio | Van Wert County, Ohio | 0.893 |
| 674 | Henderson County, Kentucky | Union County, Kentucky | 0.893 |
| 675 | Berkshire County, Massachusetts | Rensselaer County, New York | 0.892 |
| 676 | Randolph County, West Virginia | Upshur County, West Virginia | 0.892 |
| 677 | Dale County, Alabama | Houston County, Alabama | 0.892 |
| 678 | Lake County, Florida | Sumter County, Florida | 0.892 |
| 679 | Jefferson County, Florida | Wakulla County, Florida | 0.892 |
| 680 | Chase County, Kansas | Morris County, Kansas | 0.892 |
| 681 | Claiborne County, Tennessee | Grainger County, Tennessee | 0.891 |
| 682 | Letcher County, Kentucky | Wise County, Virginia | 0.891 |
| 683 | Somerset County, Pennsylvania | Westmoreland County, Pennsylvania | 0.891 |
| 684 | Braxton County, West Virginia | Clay County, West Virginia | 0.891 |
| 685 | Alleghany County, Virginia | Botetourt County, Virginia | 0.891 |
| 686 | Mississippi County, Arkansas | Pemiscot County, Missouri | 0.891 |
| 687 | Montgomery County, Arkansas | Pike County, Arkansas | 0.891 |
| 688 | Delaware County, Oklahoma | Ottawa County, Oklahoma | 0.891 |
| 689 | Montgomery County, North Carolina | Richmond County, North Carolina | 0.890 |
| 690 | Monroe County, Iowa | Wayne County, Iowa | 0.890 |
| 691 | Marshall County, Minnesota | Grand Forks County, North Dakota | 0.890 |

| | | | |
|-----|----------------------------------|-------------------------------|-------|
| 692 | Rabun County, Georgia | Clay County, North Carolina | 0.889 |
| 693 | Allegany County, Maryland | Washington County, Maryland | 0.889 |
| 694 | Franklin Parish, Louisiana | Richland Parish, Louisiana | 0.889 |
| 695 | Fergus County, Montana | Musselshell County, Montana | 0.889 |
| 696 | Jackson County, Texas | Lavaca County, Texas | 0.888 |
| 697 | Liberty County, Texas | Montgomery County, Texas | 0.888 |
| 698 | Henderson County, Texas | Smith County, Texas | 0.887 |
| 699 | Dixon County, Nebraska | Union County, South Dakota | 0.887 |
| 700 | Buchanan County, Virginia | Dickenson County, Virginia | 0.887 |
| 701 | Logan County, Colorado | Sedgwick County, Colorado | 0.887 |
| 702 | Hidalgo County, Texas | Kenedy County, Texas | 0.887 |
| 703 | Clark County, Kansas | Comanche County, Kansas | 0.887 |
| 704 | Lea County, New Mexico | Winkler County, Texas | 0.886 |
| 705 | DeKalb County, Alabama | Walker County, Georgia | 0.886 |
| 706 | Rusk County, Wisconsin | Washburn County, Wisconsin | 0.886 |
| 707 | Creek County, Oklahoma | Osage County, Oklahoma | 0.886 |
| 708 | Buckingham County, Virginia | Nelson County, Virginia | 0.886 |
| 709 | Chester County, Tennessee | Hardin County, Tennessee | 0.886 |
| 710 | Anderson County, Texas | Navarro County, Texas | 0.886 |
| 711 | Harper County, Kansas | Kingman County, Kansas | 0.886 |
| 712 | Fentress County, Tennessee | Putnam County, Tennessee | 0.885 |
| 713 | Hall County, Georgia | Jackson County, Georgia | 0.885 |
| 714 | Boyle County, Kentucky | Lincoln County, Kentucky | 0.885 |
| 715 | Monongalia County, West Virginia | Preston County, West Virginia | 0.885 |
| 716 | Bartholomew County, Indiana | Shelby County, Indiana | 0.885 |
| 717 | Johnson County, Georgia | Treutlen County, Georgia | 0.885 |
| 718 | Lamar County, Georgia | Monroe County, Georgia | 0.885 |
| 719 | Houston County, Texas | Leon County, Texas | 0.884 |
| 720 | Monroe County, Ohio | Wetzel County, West Virginia | 0.884 |
| 721 | Gilchrist County, Florida | Levy County, Florida | 0.884 |
| 722 | Madison County, North Carolina | Greene County, Tennessee | 0.884 |

TABLE S2. Reported spatial disparities in lung cancer mortality between neighboring US counties.

REFERENCES